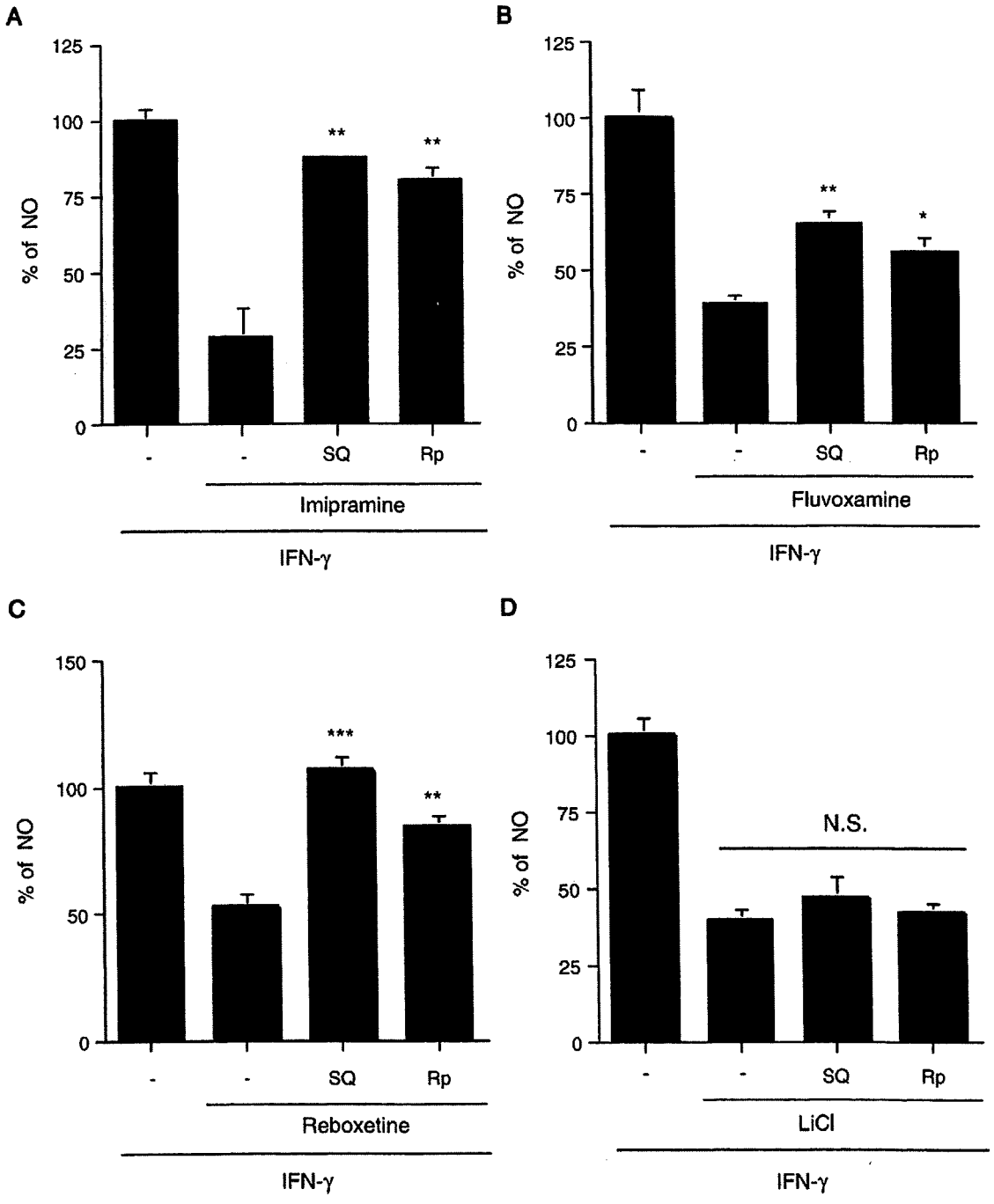

Fig. 5. Effects of cAMP/PKA inhibitors on the antidepressants-induced NO suppression. 6-3 microglial cells were pre-incubated for 20 min with SQ 22536 (10 μM) or Rp-3′,5′-cAMPS (10 μM) before the addition of imipramine (50 μM) (A), fluvoxamine (50 μM) (B), reboxetine (50 μM) (C) or lithium chloride (1 mM) (D). After 24 h of the pretreatment with antidepressants or lithium chloride, the cells were stimulated by 100 U/ml of IFN-γ. After 48 h, the media collected were assayed for NO accumulation using Griess reaction. Values are the means±SEM of 3–6 samples and expressed as percentage control, where 100% is the value obtained from IFN-γ alone. $*p<0.05$, $**p<0.01$, $***p<0.0001$, compared with imipramine (A), fluvoxamine (B), reboxetine (C) or lithium chloride (D). Comparisons were made with ANOVA followed by the Fisher's PLSD. N.S., no significance; SQ, SQ 22536; Rp, Rp-3′,5′-cAMPS.

of 50 μM. In contrast, SQ 22536 and Rp-3′,5′-cAMPS did not reverse the lithium chloride-induced NO suppression (Fig. 5D).

Discussion

Our study had four major findings. First, various types of antidepressants inhibited the IFN-γ-induced microglial production of inflammatory mediators such as IL-6 and NO. Second, these inhibitions were reversed significantly by either a cAMP inhibitor (SQ 22536) or a PKA inhibitor (Rp-3′,5′-cAMPS). Third, lithium chloride enhanced the IFN-γ-induced microglial production of IL-6, while it inhibited the production of NO. Fourth, the lithium chloride-induced NO suppression was not reversed by either SQ 22536 or Rp-3′,5′-cAMPS.

In line with the recent *ex vivo/in vitro* studies demonstrating the immunosuppressive effects of antidepressants (Kubera et al., 2001; Maes et al., 1999, 2005; Obuchowicz et al., 2006; Szuster-Ciesielska et al., 2003; Xia et al., 1996), the present study has shown that various types of antidepressants inhibit the IFN-γ-induced microglial production of both IL-6 and NO. The detailed mechanism by which antidepressants inhibit the production of pro-inflammatory mediators by immune cells, including microglia, still remains to be elucidated. However, several *ex vivo/in vitro* studies have suggested that elevated intracellular cAMP concentrations, induced by treatment with antidepressants (Xia et al., 1996), contribute to the immunosuppressive effects of antidepressants (Kubera et al., 2001; Maes et al., 2005). Consistent with these studies, our results have demonstrated that SQ 22536 and Rp-3′,5′-cAMPS reverse significantly the antidepressant-induced inhibition of microglial IL-6 and NO production. The only exception was that the effect of Rp-3′,5′-cAMPS did not reach significance for reboxetine at the concentrations used ($p=0.0558$). These results suggest that the inhibitory effects of antidepressants on IFN-γ-activated microglia are, at least partially, mediated by the cAMP-dependent PKA pathway. Indeed, in a number of cell types, the activation of cAMP/PKA pathway has been shown to inhibit the transcription factor nuclear factor-κB (Delfino and Walker, 1999), whose activation is known to induce the gene expression of inducible NO synthase and various pro-inflammatory cytokines, including IL-6 (Yoshimura, 2006).

A number of *in vivo* studies have suggested that many antidepressants increase intracellular levels of cAMP through activation of monoamine receptors such as the receptors for serotonin (5-HT), noradrenaline (NA) (Duman, 1998; Malberg and Blendy, 2005) and dopamine (Brustolim et al., 2006). Explicitly, the majority of antidepressants increase synaptic levels of 5-HT and NA through inhibiting reuptake by their transporters on presynaptic neurons, and thus cause the activation of their receptors coupled to G-proteins that can regulate the cAMP system. Through G-protein activation of adenylate cyclase (i.e., through the activation of 5-HT or NA receptor subtypes positively coupled to adenylate cyclase), cAMP production is increased. Our *in vitro* study suggests that antidepressants may have an action on microglia independently of such receptors. They may act in a monoamine receptor-independent manner. Alternatively, they may act on interferon-γ receptors or other unidentified surface receptors that are linked to G proteins. We also cannot rule out direct effects of antidepressants on G proteins.

There are also reports of pro-inflammatory effects of antidepressants, suggesting an opposite mechanism of action to our study. Specifically, it has been shown that imipramine enhances IL-6 production in human whole blood stimulated with phytohemagglutinin/LPS (Kubera et al., 2004) and that fluoxetine increases the IL-6, NO and TNF-α production when applied to unstimulated BV2 murine microglial cells (Ha et al., 2006). The effects of antidepressants on the production of pro-inflammatory mediators may therefore depend on the type of G proteins stimulated.

Another possible target of antidepressants in microglia is the phosphodiesterase (PDE) that degrades cAMP. Recently, PDE genes have been shown to be associated with a susceptibility to major depression and antidepressant treatment response (Wong et al., 2006). Accordingly, antidepressants could directly affect PDE function in microglia *in vitro* and thus increase the intracellular cAMP.

IC_{50} values of imipramine and fluvoxamine for inhibiting [^{3}H]5-HT uptake into rat cortical synaptosomes have been reported to be 500 nM and 70 nM, respectively (Inazu et al., 2001). In addition, IC_{50} values of reboxetine for inhibiting [^{3}H]NA and [^{3}H]5-HT uptake into rat hippocampal synaptosomes have been shown to be 8.5 nM and 6.9 μM, respectively (Miller et al., 2002). Compared with above-mentioned values, IC_{50} values of imipramine, fluvoxamine and reboxetine as inhibitors of microglial IL-6 production, which were calculated to be 37.0 μM, 25.6 μM and 51.5 μM, respectively, in the present study, appear to be high. The discrepancy between the aforementioned values and ours might stem from differences in the cell type and species. The other possibility is that, at the doses used for this study, antidepressants could act on some molecules other than monoamine transporters. In that case, G protein seems to be one of the potential targets of antidepressants in microglia as mentioned above.

The effects of lithium chloride on IFN-γ-induced microglial production of pro-inflammatory mediators differed considerably from antidepressants, as it enhanced IL-6 production and inhibited NO production. Our results are consistent with other studies demonstrating that lithium increased the production of pro-inflammatory cytokines such as IL-6 and TNF-α in human monocytes (Arena et al., 1997; Merendino et al., 1994). However, we demonstrated a paradoxical effect of lithium chloride in that it inhibited NO production. This inhibition was not reversed by either a cAMP inhibitor or a PKA inhibitor. These results suggest that the inhibitory effect of lithium on the microglial NO production is not mediated by the cAMP-dependent PKA pathway. Based on the dual effects of lithium chloride on microglial production of pro-inflammatory mediators, the mechanism of lithium action on IFN-γ-activated microglia appears to be complicated and needs further validation.

Several stimulants such as IFN-γ, LPS and PMA are well known to activate microglial cells. Most importantly, IFN-γ has been associated with major depression. Maes et al. (1994) have demonstrated that the IFN-γ secretion by mitogen-stimulated PBMC from patients with major depression is significantly higher than that from healthy subjects. In addition, IFN-γ has been shown to induce such depression-like behavior as decreased locomotor activity in mice (Weinberger et al., 1988). Accordingly, our experimental method using IFN-γ seems to be consistent with a possible pathophysiologic microenvironment in the brain of depressed patients.

Unlike IL-6, which has been shown to act as an inhibitory regulator of neurogenesis, NO has been indicated to have a dual role in adult neurogenesis (Cardenas et al., 2005). According to *in vivo* studies, NO produced by neuronal NO synthase (NOS) decreases neurogenesis (Moreno-Lopez et al., 2004), whereas

NO synthesized from inducible NOS and endothelial NOS stimulates neurogenesis (Reif et al., 2004; Zhu et al., 2003). NO under neuroinflammatory conditions has been shown to decrease neurogenesis *in vitro* (Covacu et al., 2006). Therefore, the precise role of NO in adult neurogenesis remains unclear. In this study NO production was used as a reliable parameter of rodent microglial activation.

In conclusion, this study demonstrates that various types of antidepressants inhibit IFN-γ-induced microglial production of pro-inflammatory mediators such as IL-6 and NO, while lithium chloride has mixed effects. The antidepressants-induced inhibitions seem to be, at least partially, mediated by the cAMP-dependent PKA pathway. These results support the view that antidepressants can inhibit microglial activation *in vitro*, raising the possibility that antidepressants indirectly promote adult neurogenesis through the inhibition of activated microglia *in vivo*.

Acknowledgments

Sincere appreciation is extended to Dr. Yoshito Mizoguchi and Dr. Tetsuaki Arai for their valuable advice and kind support. This research was supported in part by the Pacific Alzheimer Research Foundation.

References

Arena, A., Capozza, A.B., Orlando, M.E., Curro, F., Losi, E., Chillemi, S., Mesiti, M., Merendino, R.A., 1997. In vitro effects of lithium chloride on TNF alpha and IL-6 production by monocytes from breast cancer patients. J. Chemother. 9, 219–226.

Brustolim, D., Ribeiro-dos-Santos, R., Kast, R.E., Altschuler, E.L., Soares, M.B., 2006. A new chapter opens in anti-inflammatory treatments: the antidepressant bupropion lowers production of tumor necrosis factor-alpha and interferon-gamma in mice. Int. Immunopharmacol. 6, 903–907.

Cardenas, A., Moro, M.A., Hurtado, O., Leza, J.C., Lizasoain, I., 2005. Dual role of nitric oxide in adult neurogenesis. Brain Res. Brain Res. Rev. 50, 1–6.

Castanon, N., Leonard, B.E., Neveu, P.J., Yirmiya, R., 2002. Effects of antidepressants on cytokine production and actions. Brain Behav. Immun. 16, 569–574.

Covacu, R., Danilov, A.I., Rasmussen, B.S., Hallen, K., Moe, M.C., Lobell, A., Johansson, C.B., Svensson, M.A., Olsson, T., Brundin, L., 2006. Nitric oxide exposure diverts neural stem cell fate from neurogenesis towards astrogliogenesis. Stem Cells 24, 2792–2800.

De La Garza 2nd, R., 2005. Endotoxin- or pro-inflammatory cytokine-induced sickness behavior as an animal model of depression: focus on anhedonia. Neurosci. Biobehav. Rev. 29, 761–770.

Delfino, F., Walker, W.H., 1999. Hormonal regulation of the NF-κB signaling pathway. Mol. Cell. Endocrinol. 157, 1–9.

Duman, R.S., 1998. Novel therapeutic approaches beyond the serotonin receptor. Biol. Psychiatry 44, 324–335.

Duman, R.S., 2004. Depression: a case of neuronal life and death? Biol. Psychiatry 56, 140–145.

Ekdahl, C.T., Classen, J.H., Bonde, S., Kokaia, Z., Lindvall, O., 2003. Inflammation is detrimental for neurogenesis in adult brain. Proc. Natl. Acad. Sci. U. S. A. 100, 13632–13637.

Ha, E., Jung, K.H., Choe, B.K., Bae, J.H., Shin, D.H., Yim, S.V., Baik, H.H., 2006. Fluoxetine increases the nitric oxide production via nuclear factor kappa B-mediated pathway in BV2 murine microglial cells. Neurosci. Lett. 397, 185–189.

Hashioka, S., Han, Y.H., Fujii, S., Kato, T., Monji, A., Utsumi, H., Sawada, M., Nakanishi, H., Kanba, S., 2007. Phospholipids modulate superoxide and nitric oxide production by lipopolysaccharide and phorbol 12-myristate-13-acetate-activated microglia. Neurochem. Int. 50, 499–506.

Inazu, M., Takeda, H., Ikoshi, H., Sugisawa, M., Uchida, Y., Matsumiya, T., 2001. Pharmacological characterization and visualization of the glial serotonin transporter. Neurochem. Int. 39, 39–49.

Itagaki, S., McGeer, P.L., Akiyama, H., Zhu, S., Selkoe, D., 1989. Relationship of microglia and astrocytes to amyloid deposits of Alzheimer disease. J. Neuroimmunol. 24, 173–182.

Kanzawa, T., Sawada, M., Kato, M., Yamamoto, K., Mori, H., Tanaka, R., 2000. Differentiated regulation of allo-antigen presentation by different types of murine microglial cell lines. J. Neurosci. Res. 62, 383–388.

Kubera, M., Lin, A.H., Kenis, G., Bosmans, E., van Bockstaele, D., Maes, M., 2001. Anti-inflammatory effects of antidepressants through suppression of the interferon-gamma/interleukin-10 production ratio. J. Clin. Psychopharmacol. 21, 199–206.

Kubera, M., Kenis, G., Bosmans, E., Kajta, M., Basta-Kaim, A., Scharpe, S., Budziszewska, B., Maes, M., 2004. Stimulatory effect of antidepressants on the production of IL-6. Int. Immunopharmacol. 4, 185–192.

Maes, M., Scharpe, S., Meltzer, H.Y., Okayli, G., Bosmans, E., D'Hondt, P., Vanden Bossche, B.V., Cosyns, P., 1994. Increased neopterin and interferon-gamma secretion and lower availability of L-tryptophan in major depression: further evidence for an immune response. Psychiatry Res. 54, 143–160.

Maes, M., Song, C., Lin, A.H., Bonaccorso, S., Kenis, G., De Jongh, R., Bosmans, E., Scharpe, S., 1999. Negative immunoregulatory effects of antidepressants: inhibition of interferon-gamma and stimulation of interleukin-10 secretion. Neuropsychopharmacology 20, 370–379.

Maes, M., Kenis, G., Kubera, M., De Baets, M., Steinbusch, H., Bosmans, E., 2005. The negative immunoregulatory effects of fluoxetine in relation to the cAMP-dependent PKA pathway. Int. Immunopharmacol. 5, 609–618.

Malberg, J.E., Blendy, J.A., 2005. Antidepressant action: to the nucleus and beyond. Trends Pharmacol. Sci. 26, 631–638.

Malberg, J.E., Eisch, A.J., Nestler, E.J., Duman, R.S., 2000. Chronic antidepressant treatment increases neurogenesis in adult hippocampus. J. Neurosci. 20, 9104–9110.

McGeer, P.L., McGeer, E.G., 2004. Inflammation and the degenerative diseases of aging. Ann. N. Y. Acad. Sci. 1035, 104–116.

Merendino, R.A., Mancuso, G., Tomasello, F., Gazzara, D., Cusumano, V., Chillemi, S., Spadaro, P., Mesiti, M., 1994. Effects of lithium carbonate on cytokine production in patients affected by breast cancer. J. Biol. Regul. Homeost. Agents 8, 88–91.

Miller, D.B., O'Callaghan, J.P., 2005. Depression, cytokines, and glial function. Metabolism 54, 33–38.

Miller, D.K., Wong, E.H., Chesnut, M.D., Dwoskin, L.P., 2002. Reboxetine: functional inhibition of monoamine transporters and nicotinic acetylcholine receptors. J. Pharmacol. Exp. Ther. 302, 687–695.

Monje, M.L., Toda, H., Palmer, T.D., 2003. Inflammatory blockade restores adult hippocampal neurogenesis. Science 302, 1760–1765.

Moreno-Lopez, B., Romero-Grimaldi, C., Noval, J.A., Murillo-Carretero, M., Matarredona, E.R., Estrada, C., 2004. Nitric oxide is a physiological inhibitor of neurogenesis in the adult mouse subventricular zone and olfactory bulb. J. Neurosci. 24, 85–95.

Mowla, A., Mosavinasab, M., Pani, A., 2007. Does fluoxetine have any effect on the cognition of patients with mild cognitive impairment?: a double-blind, placebo-controlled, clinical trial. J. Clin. Psychopharmacol. 27, 67–70.

Obuchowicz, E., Kowalski, J., Labuzek, K., Krysiak, R., Pendzich, J., Herman, Z.S., 2006. Amitriptyline and nortriptyline inhibit interleukin-1β release by rat mixed glial and microglial cell cultures. Int. J. Neuropsychopharmacol. 9, 27–35.

Reif, A., Schmitt, A., Fritzen, S., Chourbaji, S., Bartsch, C., Urani, A., Wycislo, M., Mossner, R., Sommer, C., Gass, P., Lesch, K.P., 2004. Differential effect of endothelial nitric oxide synthase (NOS-III) on the regulation of adult neurogenesis and behaviour. Eur. J. Neurosci. 20, 885–895.

Santarelli, L., Saxe, M., Gross, C., Surget, A., Battaglia, F., Dulawa, S., Weisstaub, N., Lee, J., Duman, R., Arancio, O., Belzung, C., Hen, R., 2003. Requirement of hippocampal neurogenesis for the behavioral effects of antidepressants. Science 301, 805–809.

Schiepers, O.J., Wichers, M.C., Maes, M., 2005. Cytokines and major depression. Prog. Neuropsychopharmacol. Biol. Psychiatry 29, 201–217.

Smith, R.S., 1991. The macrophage theory of depression. Med. Hypotheses 35, 298–306.

Steiner, J., Bielau, H., Brisch, R., Danos, P., Ullrich, O., Mawrin, C., Bernstein, H.G., Bogerts, B., in press. Immunological aspects in the neurobiology of suicide: Elevated microglial density in schizophrenia and depression is associated with suicide. J. Psychiatr. Res. doi: 10.1016/j.jpsychires.2006.10.013.

Szuster-Ciesielska, A., Tustanowska-Stachura, A., Slotwinska, M., Marmurowska-Michalowska, H., Kandefer-Szerszen, M., 2003. In vitro immunoregulatory effects of antidepressants in healthy volunteers. Pol. J. Pharmacol. 55, 353–362.

Vallieres, L., Campbell, I.L., Gage, F.H., Sawchenko, P.E., 2002. Reduced hippocampal neurogenesis in adult transgenic mice with chronic astrocytic production of interleukin-6. J. Neurosci. 22, 486–492.

Weinberger, S.B., Schulteis, G., Fernando, A.G., Bakhit, C., Martinez, J.L., 1988. Decreased locomotor activity produced by repeated, but not single, administration of murine-recombinant interferon-gamma in mice. Life Sci. 42, 1085–1090.

Wong, M.L., Whelan, F., Deloukas, P., Whittaker, P., Delgado, M., Cantor, R. M., McCann, S.M., Licinio, J., 2006. Phosphodiesterase genes are associated with susceptibility to major depression and antidepressant treatment response. Proc. Natl. Acad. Sci. U. S. A. 103, 15124–15129.

Xia, Z., DePierre, J.W., Nassberger, L., 1996. Tricyclic antidepressants inhibit IL-6, IL-1 beta and TNF-alpha release in human blood monocytes and IL-2 and interferon-gamma in T cells. Immunopharmacology 34, 27–37.

Yoshimura, A., 2006. Signal transduction of inflammatory cytokines and tumor development. Cancer Sci. 97, 439–447.

Zhu, D.Y., Liu, S.H., Sun, H.S., Lu, Y.M., 2003. Expression of inducible nitric oxide synthase after focal cerebral ischemia stimulates neurogenesis in the adult rodent dentate gyrus. J. Neurosci. 23, 223–229.

N-Benzyl-2-(6,8-dichloro-2-(4-chlorophenyl)imidazo[1,2-*a*]pyridin-3-yl)-*N*-(6-(7-nitrobenzo[*c*][1,2,5]oxadiazol-4-ylamino)hexyl)acetamide as a New Fluorescent Probe for Peripheral Benzodiazepine Receptor and Microglial Cell Visualization†

Valentino Laquintana,‡ Nunzio Denora,‡ Angela Lopedota,‡ Hiromi Suzuki,§ Makoto Sawada,§ Mariangela Serra,# Giovanni Biggio,# Andrea Latrofa,‡ Giuseppe Trapani,*,‡ and Gaetano Liso‡

Dipartimento Farmaco-Chimico, Facoltà di Farmacia, Università degli Studi di Bari, Via Orabona 4, 70125 Bari, Italy, Department of Brain Function, Research Institute of Environmental Medicine, Nagoya University, Nagoya 464-8601, Japan, and Dipartimento di Biologia Sperimentale, Sezione di Neuroscienze, Università di Cagliari, Cittadella Universitaria Monserrato, SS 554 Km 4.5, Monserrato (Cagliari), Italy. Received December 20, 2006; Revised Manuscript Received July 17, 2007

The aim of this work was to develop new fluorescent probes for the localization and function of the peripheral benzodiazepine receptor (PBR). This receptor is primarily expressed on the mitochondria, and it is overexpressed in a variety of different states including glioma, breast cancer, Alzeheimer's disease, and activated microglia. For the mentioned purpose, imidazopyridine and imidazopyrimidine compounds **5**–**20** were synthesized, and their affinity for PBR was determined. Although some intrinsically fluorescent imidazopyrimidine compounds **12**–**20** possess good binding affinity, they cannot be used for visualizing PBR due to their unfavorable fluorescence characteristics. Among the imidazopyridine–7-nitrofurazan conjugates **5**–**11**, compound **10** was the most active, and it was found to stain live Ra2 microglial cells effectively. An in vivo biodistribution study carried out on compound **10** showed that this imidazopyridine derivative, injected in the carotid artery, is able to penetrate to liver parenchyma, whereas fluorescein isothiocyanate labeled dextran (FITC-dextran), used as a control dye, hardly penetrated from blood vessels to tissues. On the other hand, as for the distribution to brain, the patterns of staining with **10** and FITC-dextran are similar, indicating that both of them hardly penetrate into the brain because of the existence of the blood–brain barrier. The obtained results indicate that compound **10** represents a new useful fluorescent probe for visualization of activated microglia and PBR.

INTRODUCTION

The peripheral benzodiazepine receptor (PBR) is pharmacologically distinct from the central benzodiazepine receptor (CBR), which is coupled to GABA-regulated chloride channels in the central nervous system (CNS). CBR mediates the classical sedative, anxiolytic, anticonvulsant, and muscle relaxant properties of the benzodiazepines. On the other hand, the 18 kDa protein PBR, located in the outer mitochondrial membrane (*1*) and for which the name "translocator protein" has recently been proposed (*2*), plays an important role in stimulating the neurosteroids synthesis in glial cells, and it is involved in various neurological diseases such as Alzheimer's disease, Huntington's disease, and multiple sclerosis (*3*–*7*). In this regard, one useful index in delineating areas of active disease in the brain is the presence of activated microglia. In normal brain parenchyma, microglia are in a down-regulated state, but during disease or injury the microglia are activated and the expression of PBR in vivo is increased (*8*). Thus, the visualization of activated microglia is of relevant diagnostic value and suitable for monitoring of disease progression in the brain (*8*). There is also evidence showing that PBR expression is selectively increased in a wide variety of human tumors, including cancers of the colon, breast, ovary, liver, and especially the brain (*9*–*11*). Moreover, it has also been shown that PBR-specific ligands induce apoptosis and cell cycle arrest in cancer cells (*12*–*14*) and that appropriate PBR ligand–drug conjugates characterized by PBR affinity can be used as diagnostic imaging agents of solid tumors or to selectively release the linked anticancer drug to the target by a receptor-mediated mechanism (*15*–*18*). The synthesis and biological activity of compound **1** (Chart 1) have been reported by Kozikowski et al. (*19*), and this compound represents the first example of a fluorescent probe for PBR. Compound **1** was obtained by linking a fluorogenic 7-nitro-2,1,3-benzoxadiazol-4-yl moiety to the 2-phenylindole-3-acetic acid through a hexamethylenediamine spacer, and **1** was found to possess biological activity like other indoleacetamide PBR ligands at nanomolar levels (*19*). Moreover, by conjugation of different trifunctional lanthanide chelates to the isoquinoline PBR ligand PK11195 analogue, two conjugate compounds of general formula **2** (Chart 1) were prepared (*20*). For these conjugates, which may provide an optical or magnetic resonance (MR) signature depending on the involved lanthanide ion M (i.e., Eu^{3+} for optical or Gd^{3+} for MR), no affinity or selectivity data for PBR were provided. Subsequently, the same research group developed the molecular imaging agent **3** by conjugation of a PK11195 analogue with Lissamine–Rhodamine B dye, and the K_d of this conjugate to PBR was 1 μM (*21*). Chen et al. also reported that pyropheophorbides and their metal complexes **4** [M = In(III), Ni (II), and Zn(II)], characterized by PBR binding values at nano–micromolar levels, could be promising candidates as fluorescent probes for PBR and may have great potential as fluorophores to replace radioactive PBR probes (*22*). Further studies demonstrated that in addition to 2-phenylindole-3-acetic acid and isoquinoline derivatives (*23*, *24*), PBR binds with high affinity to other classes of compounds such as

† This work is dedicated to the memory of our colleague Prof. Gaetano Liso, recently deceased.

* Author to whom correspondence should be addressed [telephone (039) 080-5442764; fax (039) 080-5442754; e-mail trapani@farmchim.uniba.it.

‡ Università degli Studi di Bari.

§ Nagoya University.

Università di Cagliari.

10.1021/bc060393c CCC: $37.00
Published on Web 08/28/2007

Chart 1

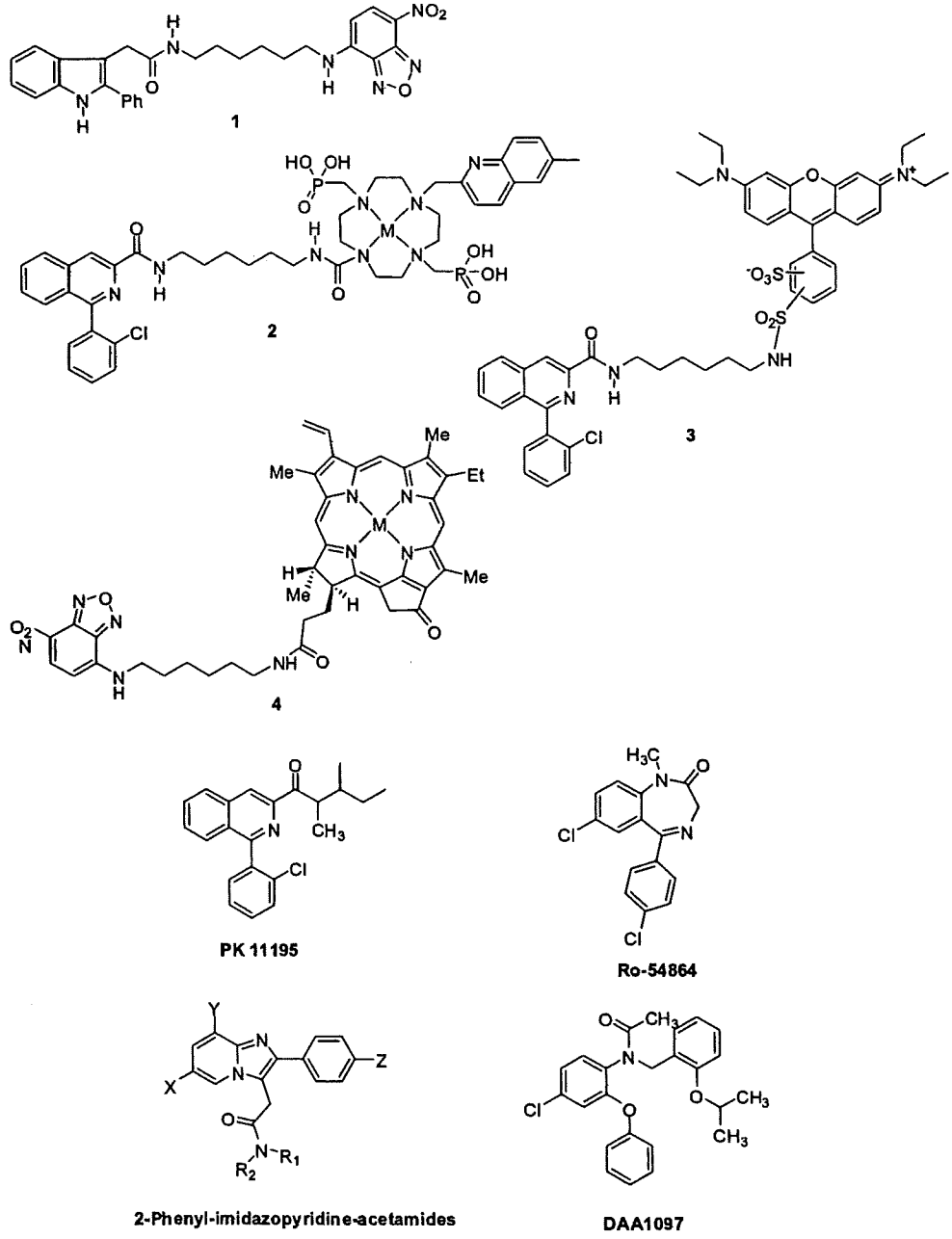

benzodiazepines (*25*) and *N*-phenoxyphenyl-*N*-isopropoxybenzyl-acetamides such as DAA1097 (*26*). We have shown that some 2-phenyl-imidazo[1,2-*a*]pyridine-3-acetamides (Chart 1) are potent and selective ligands for PBR and stimulate steroidogenesis both in the brain and at the periphery (*27*−29).

As part of our research program aimed at developing new probes for the localization and function of PBR in different tissues, we report the synthesis and biological evaluation of compounds **5**−**11** and **12**−**20** (Table 1). Compounds of the former set are characterized by a 7-nitro-2,1,3-benzoxadiazol-4-yl fluorophore linked through a diamine spacer to 2-phenylimidazo[1,2-*a*]pyridine-3-acyl moiety, whereas the other compounds may also be of interest because they are characterized by an imidazopyrimidine nucleus, which is intrinsically fluorescent (*30*) and are also analogues of imidazopyridine-3-acetamides with affinity and selectivity for PBR. Because the insertion of a bulky fluorescent group on a ligand is known to reduce binding affinity for the receptor, one might expect that compounds **12**−**20** would interact better than the conjugated compounds **5**−**11**. In this paper, the synthesis, binding data, fluorescence characteristics, and cell biology of these imidazopyridine and imidazopyrimidine compounds **5**−**20** are reported and discussed.

EXPERIMENTAL PROCEDURES

Chemistry. Melting points were determined in open capillary tubes with a Buchi apparatus and are uncorrected. IR spectra were obtained on a Perkin-Elmer 283 spectrophotometer (KBr pellets for solid or nujol for liquid). ^{1}H NMR spectra were determined on a Varian 390 or Bruker 300 MHz instrument. Chemical shifts are given in δ values downfield from Me_4Si as an internal standard. Mass spectra were recorded on a Hewlett-Packard 5995c GC-MS low-resolution spectrometer. All compounds showed appropriate IR, ^{1}H NMR, and mass spectra. Elemental analyses were performed on a Hewlett-Packard 185 C, H, N analyzer and agreed with theoretical values within ±0.40%. Silica gel 60 (Merck 70−230 mesh) was used for column chromatography. The starting 2-aminopyrimidine compounds, 4-chloro-7-nitrobenzofurazan (NBD chloride), alkyl-

Table 1. Structures and Physical Properties of Compounds 5–20

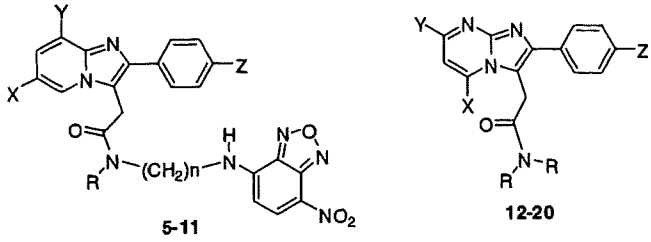

compd	R	X	Y	Z	*n*	mp (°C)	yield (%)
5	H	Cl	Cl	Cl	2	255–257	30
6	$CH_2C_6H_5$	Cl	Cl	Cl	2	250–253	35
7	H	Cl	Cl	Cl	4	155–160	44
8	$CH_2C_6H_5$	Cl	Cl	Cl	4	200–203	56
9	H	Cl	Cl	Cl	6	121–124	65
10	$CH_2C_6H_5$	Cl	Cl	Cl	6	213–215	55
11	H	Cl	Cl	H	4	212–217	45
12	C_2H_5	H	H	Cl		180–181	27
13	C_3H_7	H	H	H		115–117	20
14	C_3H_7	H	CH_3	Cl		126–128	10
15	C_3H_7	H	H	Cl		127–129	22
16	C_3H_7	H	CH_3	H		106–108	10
17	C_3H_7	CH_3	CH_3	Cl		111–113	20
18	C_4H_9	H	H	Cl		116–118	40
19	C_4H_9	H	H	H		121–123	39
20	C_6H_{13}	H	H	Cl		92–94	20

endiamines, triethylamine (TEA), ethyl 1,2-dihydro-2-ethoxy-1-quinolinecarboxylate (EEDQ), and anhydrous tetrahydrofuran (THF) were purchased from Sigma-Aldrich (Milan, Italy).

General Procedure for the Preparation of 2-Phenylimidazo[1,2-*a*]pyridineacetamide *N*-Alkylcarbamates 23a–g. To a stirred solution of the required imidazo[1,2-*a*]pyridin-3-acetic acid **21** (1 mmol) in anhydrous THF (20 mL) were added EEDQ (1.2 mmol), the appropriate mono-Boc-protected polymethylendiamine **22a–f** (1.1 mmol), and TEA (1.3 mmol) successively. Stirring was prolonged at room temperature for 6–12 h, and the resulting reaction mixture was poured into 20 mL of water (pH ~4.5) and extracted with ethyl acetate (3 × 30 mL). The organic layer was separated, washed with water and brine, and dried over Na_2SO_4. Solvent was evaporated under reduced pressure, and the resulting residue was purified by silica gel column chromatography [light petroleum ether/ethyl acetate 6:4 (v/v) as eluent)] to give the corresponding compounds **23a–g**.

tert-Butyl-2-(2-(6,8-dichloro-2-(4-chlorophenyl)imidazo[1,2-a]pyridin-3-yl)acetamido)ethylcarbamate (23a): IR (KBr) 3340, 1681, 1640 cm^{-1}; ^1H NMR ($CDCl_3$) δ 1.36 (s, 9H, $C(CH_3)_3$), 3.2–3.3 (m, 2H, CH_2N-Boc), 3.3–3.4 (m, 2H, CH_2NCO), 3.92 (s, 2H, CH_2CO), 4.85 (br 1H, NH-Boc), 7.00 (br 1H, NH–CO), 7.35 (s, 1H, Ar), 7.43 (d, J = 8.2 Hz, 2H, Ar), 7.69 (d, J = 8.2 Hz, 2H, Ar), 8.22 (s, 1H, Ar); MS (ESI) m/z 497 (M + H)$^+$. Anal. ($C_{22}H_{23}Cl_3N_4O_3$) C, H, N.

tert-Butyl-2-(N-benzyl-2-(6,8-dichloro-2-(4-chlorophenyl)imidazo[1,2-a]pyridin-3-yl)acetamido)ethylcarbamate (23b): IR (KBr) 3345, 1710, 1631 cm^{-1}; ^1H NMR ($CDCl_3$) δ 1.44 (s, 9H, $C(CH_3)_3$), 3.1–3.6 (m, 4H, CH_2N-Boc and CH_2NCO), 4.01 (s, 1.4H, CH_2CO), 4.17 (s, 0.6H, CH_2CO), 4.55 (s, 1.4H, CH_2-Ar), 4.64 (s, 0.6H, CH_2Ar), 4.8–4.9 (br 1H, NH), 7.0–7.5 (m, 10H, Ar), 8.62 (m, 0.4H, Ar), 8.19 (m, 0.6H, Ar); MS (ESI) m/z 589 (M + H)$^+$. Anal. ($C_{29}H_{29}Cl_3N_4O_3$) C, H, N.

tert-Butyl-4-(2-(6,8-dichloro-2-(4-chlorophenyl)imidazo[1,2-a]pyridin-3-yl)acetamido)butylcarbamate (23c): IR (KBr) 3340, 3270, 1687, 1647 cm^{-1}; ^1H NMR (DMSO-d_6) δ 1.34 (s, 9H, $C(CH_3)_3$), 1.4–1.5 (m, 4H, CH_2CH_2), 2.8–3.0 (m, 2H, CH_2N-Boc) 3.0–3.1 (m, 2H, CH_2NCO), 4.00 (s, 2H, CH_2CO), 0.4.8 (br 1H, NH–CO), 6.80 (br 1H, NH-Boc), 7.53 (d, J = 8.5 Hz, 2H, Ar), 7.67 (d, J = 1.6 Hz, 1H, Ar), 7.79 (d, J = 8.5 Hz, 2H, Ar), 8.70 (d, J = 1.6 Hz, 1H, Ar); MS (ESI) m/z 525 (M + H)$^+$. Anal. ($C_{24}H_{27}Cl_3N_4O_3$) C, H, N.

tert-Butyl-4-(N-benzyl-2-(6,8-dichloro-2-(4-chlorophenyl)imidazo[1,2-a]pyridin-3-yl)acetamido)butylcarbamate (23d): IR (KBr) 3360, 1691, 1634 cm^{-1}; ^1H NMR ($CDCl_3$) δ 1.42 (s, 9H, $C(CH_3)_3$), 1.5–1.6 (m, 4H CH_2CH_2), 3.0–3.2 (m, 2H, CH_2N-Boc) 3.4–3.8 (m, 2H, CH_2NCO), 4.01 (s, 0.8H, CH_2-CO), 4.12 (s, 1.2H, CH_2CO), 4.45 (s, 0.8H, CH_2Ar), 4.59 (s, 1.2H, CH_2Ar), 6.9–7.7 (m, 10H, Ar), 8.11 (m, 0.9H, Ar), 8.24 (m, 0.1H, Ar); MS (ESI) m/z 617 (M + H)$^+$. Anal. ($C_{31}H_{33}Cl_3N_4O_3$) C, H, N.

tert-Butyl-6-(2-(6,8-dichloro-2-(4-chlorophenyl)imidazo[1,2-a]pyridin-3-yl)acetamido)hexylcarbamate (23e): IR (KBr) 3322, 3083, 1685, 1639 cm^{-1}; ^1H NMR ($CDCl_3$) δ 1.40 (s, 9H, $C(CH_3)_3$), 1.2–1.5 (m, 8H, CH_2), 3.0–3.1 (m, 2H, CH_2N-Boc) 3.2–3.3 (m, 2H, CH_2NCO), 3.93 (s, 2H, CH_2CO), 4.5 (br 1H, NH-Boc), 6.2 (br 1H, NH–CO), 7.33 (d, J = 1.6 Hz, 1H, Ar), 7.43 (d, J = 8.2 Hz, 2H, Ar), 7.69 (d, J = 8.2 Hz, 2H, Ar), 8.14 (d, J = 1.6 Hz, 1H, Ar); MS (ESI) m/z 555 (M + H)$^+$. Anal. ($C_{26}H_{31}Cl_3N_4O_3$) C, H, N.

tert-Butyl-6-(N-benzyl-2-(6,8-dichloro-2-(4-chlorophenyl)imidazo[1,2-a]pyridin-3-yl)acetamido)hexylcarbamate (23f): IR (KBr) 3350, 1705, 1639 cm^{-1}; ^1H NMR ($CDCl_3$) δ 1.43 (s, 9H, $C(CH_3)_3$), 1.2–1.4 (m, 4H CH_2) 1.6–1.8 (m, 4H CH_2), 3.0–3.2 (m, 2H, CH_2N-Boc) 3.4–3.5 (m, 2H, CH_2NCO), 4.00 (s, 1H, CH_2CO), 4.01 (s, 1H, CH_2CO), 4.43 (s, 1H, CH_2Ar), 4.57 (s, 1H, CH_2Ar), 4.5 (br, 1H, NH), 6.9–7.6 (m, 10H, Ar), 8.10 (m, 0.6H, Ar), 8.25 (m, 0.4H, Ar); MS (ESI) m/z 645 (M + H)$^+$. Anal. ($C_{33}H_{37}Cl_3N_4O_3$) C, H, N.

tert-Butyl-4-(2-(6,8-dichloro-2-phenyl)imidazo[1,2-a]pyridin-3-yl)acetamido)butylcarbamate (23g): IR (KBr) 3342, 1683, 1635 cm^{-1}; ^1H NMR ($CDCl_3$) δ 1.41 (s, 9H, $C(CH_3)_3$), 1.4–1.5 (m, 4H, CH_2CH_2), 3.0–3.2 (m, 2H, CH_2N-Boc) 3.2–3.4 (m, 2H, CH_2NCO), 3.95 (s, 2H, CH_2CO), 4.5–4.6 (br 1H, NH-Boc), 6.1–6.3 (br 1H, NH–CO), 7.32 (d, J = 1.6 Hz, 1H, Ar), 7.3–7.5 (m, 3H, Ar), 7.73 (d, J = 8.5 Hz, 2H, Ar), 8.15 (d, J = 1.6 Hz, 1H, Ar); MS (ESI) m/z 491 (M + H)$^+$. Anal. ($C_{24}H_{28}Cl_2N_4O_3$) C, H, N.

General Procedure for the Preparation of *N*-Aminoalkyl-2-phenylimidazo[1,2-*a*]pyridineacetamides 24a–g. In a stirred and ice-cooled solution of the appropriate carbamate **23** (0.5 mmol) in dichloromethane (20 mL) was bubbled HCl gas for 30 min. Evaporation of the solvent under reduced pressure gave the corresponding Boc-deprotected compound **24** as hydrochloride salt in good yield.

N-(2-Aminoethyl)-2-(6,8-dichloro-2-(4-chlorophenyl)imidazo-[1,2-a]pyridin-3-yl)acetamide (24a): IR (KBr) 3285, 1685 cm^{-1}; ^1H NMR (DMSO-d_6) δ 2.8–2.9 (m, 2H, CH_2N), 3.3–3.4 (m, 2H, CH_2NCO), 4.06 (s, 2H, CH_2CO), 5.2 (br 2H, NH_2), 7.54 (d, J = 8.5 Hz, 2H, Ar), 7.70 (d, J = 1.6 Hz, 1H, Ar), 7.78 (d, J = 8.5 Hz, 2H, Ar), 8.44 (m, 1H, NHCO), 8.69 (d, J = 1.6 Hz 1H, Ar); MS (ESI) m/z 397 (M + H)$^+$. Anal. ($C_{17}H_{15}Cl_3N_4O$) C, H, N.

N-(2-Aminoethyl)-2-(6,8-dichloro-N-benzyl-2-(4-chlorophenyl)imidazo[1,2-a]pyridin-3-yl)acetamide (24b): IR (KBr) 3370, 1638 cm^{-1}; ^1H NMR ($CDCl_3$) δ 2.8–2.9 (m, 4H, CH_2N and NH_2), 3.3–3.4 (m, 2H, CH_2NCO), 3.72 (s, 2H, CH_2CO), 3.89 (s, 2H, CH_2Ar), 7.2–7.4 (m, 8H, Ar), 7.76 (d, J = 8.5 Hz, 2H, Ar), 8.17 (d, J = 1.4 Hz, 1H, Ar); MS (ESI) m/z 487 (M + H)$^+$. Anal. ($C_{24}H_{21}Cl_3N_4O$) C, H, N.

N-(4-Aminobutyl)-2-(6,8-dichloro-2-(4-chlorophenyl)imidazo-[1,2-a]pyridin-3-yl)acetamide (24c): IR (KBr) 3444, 1662 cm^{-1}; ^1H NMR ($CDCl_3$) δ 1.4–1.6 (m, 6H, CH_2CH_2 and NH_2), 2.5–2.6 (m, 2H, CH_2NCO), 3.2–3.3 (m, 2H, CH_2N), 3.92 (s, 2H, CH_2CO), 7.33 (d, J = 1.6 Hz, 1H, Ar), 7.44 (d, J = 8.5 Hz, 2H, Ar), 7.3–7.4 (m, 1H, NHCO), 7.70 (d, J = 8.5 Hz, 2H,

Ar), 8.15 (d, J = 1.6 Hz 1H, Ar); MS (ESI) m/z 425 $(M + H)^+$. Anal. ($C_{19}H_{19}Cl_3N_4O$) C, H, N.

*N-(4-Aminobutyl)-2-(6,8-dichloro-N-benzyl-2-(4-chlorophenyl)imidazo[1,2-a]pyridin-3-yl)acetamide (**24d**):* IR (KBr) 3370, 1625 cm^{-1}; ^1H NMR ($CDCl_3$) δ 1.2−1.4 (m, 4H, CH_2CH_2), 1.5−1.8 (m, 2H, NH_2), 2.5−2.8 (m, 2H, CH_2N), 3.1−3.5 (m, 2H, CH_2NCO), 4.01 (s, 1.2H, CH_2CO), 4.12 (s, 0.8H, CH_2CO), 4.45 (s, 1.2H, CH_2Ar), 4.59 (s, 0.8H, CH_2Ar), 6.9−7.7 (m, 10H, Ar), 8.11 (d, J = 1.6 Hz, 0.6H, Ar), 8.27 (d, J = 1.6 Hz, 0.4H, Ar); MS (ESI) m/z 515 $(M + H)^+$. Anal. ($C_{26}H_{25}Cl_3N_4O$) C, H, N.

*N-(6-Aminohexyl)-2-(6,8-dichloro-2-(4-chlorophenyl)imidazo[1,2-a]pyridin-3-yl)acetamide (**24e**):* IR (KBr) 3442, 1636 cm^{-1}; ^1H NMR ($CDCl_3$) δ 1.2−1.6 (m, 10H, CH_2 and NH_2), 2.64 (t, J = 6.4 Hz, 2H, CH_2NCO), 3.24 (q, J = 6.4 Hz, 2H, CH_2N), 3.91 (s, 2H, CH_2CO), 5.8 (br, 1H, NHCO),7.34 (d, J = 1.6 Hz, 1H, Ar), 7.44 (d, J = 8.2 Hz, 2H, Ar), 7.68 (d, J = 8.2 Hz, 2H, Ar), 8.10 (d, J = 1.6 Hz 1H, Ar); MS (ESI) m/z 455 $(M + H)^+$. Anal. ($C_{21}H_{23}Cl_3N_4O$) C, H, N.

*N-(6-Aminohexyl)-2-(6,8-dichloro-N-benzyl-2-(4-chlorophenyl)imidazo[1,2-a]pyridin-3-yl)acetamide (**24f**):* IR (KBr) 3223, 1625 cm^{-1}; ^1H NMR ($CDCl_3$) δ 1.2−1.4 (m, 6H, CH_2 and NH_2), 1.6−1.8 (m, 4H, CH_2), 3.12 (m, 2H, CH_2N), 3.44 (m, 2H, CH_2NCO), 4.00 (s, 1H, CH_2CO), 4.10 (s, 1H, CH_2CO), 4.43 (s, 1H, CH_2Ar), 4.53 (s, 1H, CH_2Ar), 6.9−7.6 (m, 10H, Ar), 8.10 (d, J = 1.6 Hz, 0.6H, Ar), 8.25 (d, J = 1.6 Hz, 0.4H, Ar); MS (ESI) m/z 545 $(M + H)^+$. Anal. ($C_{28}H_{29}Cl_3N_4O$) C, H, N.

*N-(4-Aminobutyl)-2-(6,8-dichloro-2-phenylimidazo[1,2-a]pyridin-3-yl)acetamide (**24g**):* IR (KBr) 3471, 1641 cm^{-1}; ^1H NMR ($CDCl_3$) δ 1.2−1.6 (m, 4H, CH_2CH_2) 1.6−1.7 (br, 2H, NH_2), 2.55 (m, 2H, CH_2NCO), 3.25 (m, 2H, CH_2N), 3.96 (s, 2H, CH_2CO), 7.33 (d, J = 1.6 Hz, 1H, Ar), 7.4−7.5 (m, 3H, Ar), 7.74 (m, 2H, Ar), 8.18 (d, J = 1.6 Hz, 1H, Ar), 8.15 (d, J = 1.6 Hz 1H, Ar); MS (ESI) m/z 391 $(M + H)^+$. Anal. ($C_{19}H_{20}Cl_2N_4O$) C, H, N.

General Procedure for the Preparation of Benzooxadiazole-imidazopyridine Acetamides 5−11. To a stirred and ice-cooled solution of the appropriate compound **24a−g** (0.5 mmol) in anhydrous THF (20 mL) were added a solution of NBD chloride (0.5 mmol) in anhydrous THF (2 mL) and then TEA (0.7 mmol). Stirring was prolonged at room temperature for 1 h, and the resulting mixture was poured into 20 mL of water and then extracted with chloroform (3 × 30 mL). The organic layer was washed with water and brine and successively dried over Na_2SO_4. Solvent was evaporated under reduced pressure, and the resulting residue was purified by silica gel column chromatography [light petroleum ether/ethyl acetate 4:6 (v/v) as eluent)] to give the corresponding compounds **5−11**.

*2-(6,8-Dichloro-2-(4-chlorophenyl)imidazo[1,2-a]pyridin-3-yl)-N-(2-(7-nitrobenzo[c](1,2,5)oxadiazol-4-ylamino)ethyl)acetamide (**5**):* IR (KBr) 3250, 1656 cm^{-1}; ^1H NMR (acetone-d_6) δ 3.6−3.8 (m, 4H, NCH_2CH_2N), 4.18 (s, 2H, CH_2CO), 6.44 (d, J = 8.8 Hz, 1H, C(5)H NBD moiety), 7.4−7.5 (m, 3H, Ar), 7.87 (d, J = 8.5 Hz, 2H, Ar), 8.45 (d, J = 8.8 Hz, 1H, C(6)H of NBD moiety), 8.51 (d, J = 1.6 Hz 1H, Ar); MS (ESI) m/z 562 $(M + H)^+$. Anal. ($C_{23}H_{16}Cl_3N_7O_4$) C, H, N.

*N-Benzyl-2-(6,8-dichloro-2-(4-chlorophenyl)imidazo[1,2-a]pyridin-3-yl)-N-(2-(7-nitrobenzo[c](1,2,5)oxadiazol-4-ylamino)ethyl)acetamide (**6**):* IR (KBr) 3420, 1640 cm^{-1}; ^1H NMR (DMSO-d_6) δ 3.2−3.3 (m, 4H, NCH_2CH_2N), 3.6−4.9 (m, 4H, CH_2CO and CH_2Ar), 6.3−6.9 (m, 1H, C(5)H of NBD moiety), 7.1−7.8 (m, 10H, Ar), 8.2−8.9 (m, 2H, Ar and C(6)H of NBD moiety), 9.2−9.4 (m, 1H, NH); MS (ESI) m/z 652 $(M + H)^+$. Anal. ($C_{30}H_{22}Cl_3N_7O_4$) C, H, N.

*2-(6,8-Dichloro-2-(4-chlorophenyl)imidazo[1,2-a]pyridin-3-yl)-N-(4-(7-nitrobenzo[c](1,2,5)oxadiazol-4-ylamino)butyl)acetamide (**7**):* IR (KBr) 3280, 1658 cm^{-1}; ^1H NMR (DMSO-d_6) δ 1.4−1.5 (m, 2H, CH_2), 1.5−1.7 (m, 2H, CH_2), 3.1−3.4 (m, 4H, CH_2N), 3.73 (s, 2H, CH_2CO), 5.96 (d, J = 9.1 Hz, 1H, C(5)H NBD moiety), 7.08 (d, J = 1.6 Hz 1H, Ar), 7.22 (d, J = 8.5 Hz, 2H, Ar), 7.62 (d, J = 8.5 Hz, 2H, Ar), 7.7−7.8 (m, 1H, NH), 8.14 (d, J = 1.6 Hz 1H, Ar), 8.23 (d, J = 9.1 Hz, 1H, C(6)H of NBD moiety), 8−5-8.6 (m, 1H, NH); MS (ESI) m/z 586 $(M - H)^-$. Anal. ($C_{25}H_{20}Cl_3N_7O_4$) C, H, N.

*N-Benzyl-2-(6,8-dichloro-2-(4-chlorophenyl)imidazo[1,2-a]pyridin-3-yl)-N-(4-(7-nitrobenzo[c](1,2,5)oxadiazol-4-ylamino)butyl)acetamide (**8**):* IR (KBr) 3400, 1645 cm^{-1}; ^1H NMR (DMSO-d_6) δ 1.0−1.2 (m, 4H, CH_2CH_2), 3.0−3.3 (m, 2H CH_2N) 4.0−4.1 (m, 2H, CH_2NCO), 4.23 (s, 1H, CH_2CO), 4.41 (s, 1H, CH_2CO) 4.55 (s, 1.1H, CH_2Ar), 4.73 (s, 0.9H, CH_2Ar), 6.36 (d, 1H, C(5)H of NBD moiety), 7.1−7.7 (m, 10H, Ar), 8.2−8.7 (m 2H, Ar and C(6)H of NBD moiety), 9.5 (br, 1H, NH); MS (ESI) m/z 676 $(M - H)^-$. Anal. ($C_{32}H_{26}Cl_3N_7O_4$) C, H, N.

*2-(6,8-Dichloro-2-(4-chlorophenyl)imidazo[1,2-a]pyridin-3-yl)-N-(6-(7-nitrobenzo[c](1,2,5)oxadiazol-4-ylamino)hexyl)acetamide (**9**):* IR (KBr) 3373, 1656 cm^{-1}; ^1H NMR (DMSO-d_6) δ 1.2−1.5 (m, 6H, CH_2), 1.5−1.7 (m, 2H, CH_2), 3.0−3.1 (m, 2H, CH_2N), 3.2−3.3 (m, 2H, CH_2NCO), 4.01 (s, 2H, CH_2CO), 6.32 (d, J = 9.3 Hz, 1H, C(5)H NBD moiety), 7.49 (d, J = 8.5 Hz, 2H, Ar), 7.63 (d, J = 1.6 Hz 1H, Ar), 7.82 (d, J = 8.5 Hz, 2H, Ar), 8.3−8.4 (m, 1H, NH), 8.44 (d, J = 9.3 Hz, 1H, C(6)H of NBD moiety), 8.68 (d, J = 1.6 Hz 1H, Ar), 8.5 (br, 1H, NH); MS (ESI) m/z 614 $(M - H)^-$. Anal. ($C_{27}H_{24}Cl_3N_7O_4$) C, H, N.

*N-Benzyl-2-(6,8-dichloro-2-(4-chlorophenyl)imidazo[1,2-a]pyridin-3-yl)-N-(6-(7-nitrobenzo[c](1,2,5)oxadiazol-4-ylamino)hexyl)acetamide (**10**):* IR (KBr) 3223, 1643 cm^{-1}; ^1H NMR (DMSO-d_6) δ 1.2−1.4 (m, 4H, CH_2), 1.6−1.8 (m, 4H, CH_2), 3.0−3.2 (m, 2H CH_2N) 3.4−3.5 (m, 2H, CH_2NCO), 4.23 (s, 0.9H, CH_2CO), 4.37 (s, 1.1H, CH_2CO) 4.52 (s, 1.1H, CH_2Ar), 4.73 (s, 0.9H, CH_2Ar), 6.3−6.5 (m, 1H, C(5)H of NBD moiety), 6.9−7.6 (m, 10H, Ar), 8.43 (d, J = 9.0 Hz, 1H, C(6)H of NBD moiety), 8.56 (m, 0.4H, Ar), 8.66 (m, 0.6H, Ar), 9.5 (br, 1H, NH); MS (ESI) m/z 706 $(M + H)^+$. Anal. ($C_{34}H_{30}Cl_3N_7O_4$) C, H, N.

*2-(6,8-Dichloro-2-phenylimidazo[1,2-a]pyridin-3-yl)-N-(4-(7-nitrobenzo[c](1,2,5)oxadiazol-4-ylamino)butyl)acetamide (**11**):* IR (KBr) 3250, 1667 cm^{-1}; ^1H NMR (DMSO-d_6) δ 1.5−1.7 (m, 4H, CH_2CH_2), 3.3−3.5 (m, 2H, CH_2N), 4.02 (s, 2H, CH_2CO), 4.1−4.3 (m, 2H, CH_2NCO), 6.35 (d, J = 8.9 Hz, 1H, C(5)H NBD moiety), 6.6−6.7 (m, 1H, NH), 7.3−7.5 (m 4H, Ar), 7.61 (d, J = 1.6 Hz, 1H, Ar), 7.76 (d, J = 8.5 Hz, 2H, Ar), 8.3−8.4 (m, 1H, NH), 8.39 (d, J = 9.1 Hz, 1H, C(6)H of NBD moiety); MS (ESI) m/z 554 $(M + H)^+$; 552 $(M - H)^-$. Anal. ($C_{25}H_{21}Cl_2N_7O_4$) C, H, N.

General Procedure for the Preparation of *N,N*-Di-*n*-alkyl-(2-phenylimidazo[1,2-*a*]pyrimidin-3-yl)acetamides 12−20. To a stirred solution of the appropriate substituted 2-aminopyrimidine **27** (10 mmol) in 40 mL of DMF was added the required *N,N*-dialkyl-3-bromo-3-benzoylpropionamide **28** (10 mmol). The reaction mixture was refluxed for 6−9 h by monitoring the reaction progress on silica TLC plates [petroleum ether/ethyl acetate 1:1 (v/v) as eluent]. The solvent was removed by distillation under reduced pressure, and the resulting residue was purified by silica gel column chromatography [petroleum ether/ethyl acetate 1:1 (v/v) as eluent] to give the corresponding products **12−20**, which were crystallized from a petroleum ether/ethyl acetate mixture.

*N,N-Diethyl[2-(4-chlorophenyl)imidazo[1,2-a]pyrimidin-3-yl]-acetamide (**12**):* IR (KBr) 1645 cm^{-1}; ^1H NMR ($CDCl_3$) δ 0.9−1.2 (m, 6H, CH_3), 3.1−3.6 (m, 4H, CH_2), 4.15 (s, 2H, CH_2), 6.86 (m, 1H, Ar), 7.42 (d, J = 8.5 Hz, 2H, Ar), 7.70 (d, 2H,

Ar), 8.5−8.8 (m, 2H, Ar); MS *m/z* 342 (M^+ 25), 242 (base). Anal. ($C_{18}H_{19}ClN_4O$) C, H, N.

N,N-Di-n-propyl(2-phenylimidazo[1,2-a]pyrimidin-3-yl)acetamide (13): MS *m/z* 336 (M^+ 23), 208 (base). Anal. ($C_{20}H_{24}N_4O$) C, H, N.

N,N-Di-n-propyl[2-(4-chlorophenyl)-7-methylimidazo[1,2-a]pyrimidin-3-yl]acetamide (14): IR (KBr) 1630 cm^{-1}; ^1H NMR ($CDCl_3$) δ 0.63 (t, J = 7.3 Hz, 3H, CH_3), 0.79 (t, 3H, CH_3), 1.3−1.5 (m, 4H, CH_2), 2.61 (s, 3H, CH_3), 2.9−3.0 (m, 2H, CH_2N), 3.1−3.2 (m, 2H, CH_2N), 4.08 (s, 2H, CH_2CO), 6.70 (d, J = 7.0 Hz, 1H, Ar), 7.42 (d, J = 8.6 Hz, 2H, Ar), 7.65 (d, J = 8.6 Hz, 2H, Ar),8.55 (d, 1H, Ar); MS *m/z* 384 (M^+ 18), 256 (base). Anal. ($C_{21}H_{25}ClN_4O$) C, H, N.

N,N-Di-n-propyl[2-(4-chlorophenyl)imidazo[1,2-a]pyrimidin-3-yl]acetamide (15): IR (KBr) 1650 cm^{-1}; ^1H NMR ($CDCl_3$) δ 0.65 (t, J = 7.3 Hz, 3H, CH_3), 0.79 (t, J = 7.3 Hz, 3H, CH_3), 1.3−1.5 (m, 4H, CH_2), 2.9−3.0 (m, 2H, CH_2N), 3.1−3.2 (m, 2H, CH_2N), 4.08 (s, 2H, CH_2CO), 6.7−6.9 (m, 1H, Ar), 7.4−7.7 (m, 4H, Ar), 8.48 (m, 1H, Ar), 8.61 (d, J = 6.6 Hz, 1H, Ar); MS *m/z* 370 (M^+ 28), 242 (base). Anal. ($C_{20}H_{23}ClN_4O$) C, H, N.

N,N-Di-n-propyl(2-phenyl-7-methylimidazo[1,2-a]pyrimidin-3-yl)acetamide (16): IR (KBr) 1655 cm^{-1}; ^1H NMR ($CDCl_3$) δ 0.59 (t, J = 7.4 Hz, 3H, CH_3), 0.78 (t, J = 7.4 Hz, 3H, CH_3), 1.3−1.5 (m, 4H, CH_2), 2.60 (s, 3H, CH_3), 2.9−3.0 (m, 2H, CH_2N), 3.2−3.3 (m, 2H, CH_2N), 4.15 (s, 2H, CH_2CO), 6.7−6.8 (m, 1H, Ar), 7.3−7.5 (m, 3H, Ar), 7.7 (d, J = 7.2 Hz, 2H, Ar), 8.67 (d, 1H, Ar); MS *m/z* 350 (M^+ 19), 222 (base). Anal. ($C_{21}H_{26}N_4O$) C, H, N.

N,N-Di-n-propyl[2-(4-chlorophenyl)-5,7-dimethylimidazo[1,2-a]pyrimidin-3-yl]acetamide (17): IR (KBr) 1645 cm^{-1}; ^1H NMR ($CDCl_3$) δ 0.8−1.0 (m, 6H, CH_3), 1.5−1.7 (m, 4H, CH_2), 2.52 (s, 3H, CH_3), 2.74 (s, 3H, CH_3), 3.2−3.4 (m, 4H, CH_2N), 4.12 (s, 2H, CH_2CO), 6.46 (s, 1H, Ar), 7.3−7.6 (m, 4H, Ar); MS *m/z* 398 (M^+ 10), 270 (base). Anal. ($C_{22}H_{27}ClN_4O$) C, H, N.

N,N-Di-n-butyl[2-(4-chlorophenyl)imidazo[1,2-a]pyrimidin-3-yl]acetamide (18): IR (KBr) 1627 cm^{-1}; ^1H NMR ($CDCl_3$) δ 0.8−1.0 (m, 6H, CH_3), 1.2−1.6 (m, 8H, CH_2), 3.1−3.5 (m, 4H, CH_2N), 4.20 (s, 2H, CH_2CO), 6.9−7.1 (m, 1H, Ar), 7.4−7.8 (m, 4H, Ar), 8.6−8.9 (m, 2H, Ar); MS *m/z* 398 (M^+ 31), 242 (base). Anal. ($C_{22}H_{27}ClN_4O$) C, H, N.

N,N-Di-n-butyl(2-phenylimidazo[1,2-a]pyrimidin-3-yl)acetamide (19): IR (KBr) 1630 cm^{-1}; ^1H NMR ($CDCl_3$) δ 0.7−1.0 (m, 6H, CH_3), 1.2−1.6 (m, 8H, CH_2), 2.9−3.4 (m, 4H, CH_2N), 4.15 (s, 2H, CH_2CO), 6.8−6.9 (m, 1H, Ar), 7.3−7.8 (m, 5H, Ar), 8.5−8.8 (m, 2H, Ar); MS *m/z* 364 (M^+ 24), 208 (base). Anal. ($C_{22}H_{28}N_4O$) C, H, N.

N,N-Di-n-hexyl[2-(4-chlorophenyl)imidazo[1,2-a]pyrimidin-3-yl]acetamide (20): IR (KBr) 1645 cm^{-1}; ^1H NMR ($CDCl_3$) δ 0.8−0.9 (m, 6H, CH_3), 1.1−1.5 (m, 16H, CH_2), 2.9−3.1 (m, 2H, CH_2N), 3.2−3.3 (m, 2H, CH_2N), 4.09 (s, 2H, CH_2CO), 6.8−6.9(m, 1H, Ar), 7.42 (d, J = 8.5 Hz, 2H, Ar), 7.63 (d, J = 8.5 Hz, 2H, Ar), 8.5−8.6 (m, 1H, Ar), 8.6−8.7 (m, 1H, Ar); MS *m/z* 454 (M^+ 21), 242 (base). Anal. ($C_{26}H_{35}ClN_4O$) C, H, N.

Stability Studies on Compound 10. *Chemical Hydrolysis.* Stability studies were carried out at controlled temperature (37 ± 0.2 °C) in a water bath shaken at 150 rpm. The hydrolysis of compound **10** was studied at pH 7.4 in isotonic 0.05 M phosphate buffer. The experiments were carried out by adding 35 μL of a stock solution in DMSO (1.0 mg/mL) to 1 mL of the buffer solution preheated at 37 °C. The final concentration of the resulting solutions was 50 μM. The test solutions were vortexed and maintained in a shaker water bath at a constant temperature of 37 ± 0.2 °C. At appropriate intervals, aliquots of 20 μL were removed and immediately analyzed by high-performance liquid chromatography (HPLC). Pseudo-first-order rate constants for the hydrolysis of the derivatives were determined from the slopes of linear plots of the logarithms of residual compound against time. HPLC analyses were performed with a Waters Associates model 600 pump equipped with a Waters 990 variable wavelength UV detector and a 20 μL loop injection valve. A reversed phase Symmetry C18 (25 cm × 3.9 mm; 5 μm particles) column in conjunction with a precolumn (Sentry Guard Symmetry C18, 20 × 3.9 mm) was eluted with mixtures of methanol/water 80:20 (v/v). The injected volume was 20 μL. The flow rate of 0.8 mL/min was maintained, and the column effluent was monitored continuously at 254 nm. The compounds were estimated by measuring the peak areas or peak heights in relation to those of standards chromatographed under the same conditions.

Stability in Physiological Medium. The stability of compound **10** in physiological medium was studied at 37 °C in 0.05 M phosphate buffer saline (0.14 M NaCl) at pH 7.4, containing 50% v/v of rat serum. The final concentration was 50 μM. The resulting test solution was maintained at 37 ± 0.2 °C in a shaking water bath. Aliquots of 100 μL were withdrawn at appropriate intervals and treated with 500 μL of cold acetonitrile to precipitate the serum proteins. After mixing and centrifugation for 5 min at 13200 rpm, the clear supernatant was analyzed by HPLC as described above.

Biological Methods and Materials. Adult male or female Sprague−Dawley CD rats (Charles River, Como, Italy) with body masses of 200−250 g at the beginning of the experiments were maintained under an artificial 12-h light/dark cycle (light on from 8:00 a.m. to 8:00 p.m.) at a constant temperature of 23 ± 2 °C and 65% humidity. Food and water were freely available, and the animals were acclimated for >7 days before use. Experiments were performed between 8:00 a.m. and 2:00 p.m. Animal care and handling throughout the experimental procedure were performed in accordance with the European Communities Council Directive of 24 November 1986 (86/609/EEC). The experimental protocols were approved by the Animal Ethical Committee of the University of Cagliari.

In Vitro Receptor Binding Assays. After sacrifice, the brain was rapidly removed and the cerebral cortex was dissected; tissues were stored at −80 °C until assay.

[^{3}H]Flunitrazepam Binding. The tissues were thawed and homogenized with a Polytron PT 10 in 50 volumes of ice-cold 50 mM Tris-HCl buffer (pH 7.4) and centrifuged twice at 20000*g* for 10 min. The pellet was reconstituted in 50 volumes of Tris-HCl buffer and was used for the binding assay. Aliquots of 400 μL of tissue homogenate (0.4−0.5 mg of protein) were incubated in the presence of [^{3}H]flunitrazepam at a final concentration of 0.5 nM, in a total incubation volume of 1000 μL. The drugs were added in 100 μL aliquots. After a 60 min incubation at 0 °C, the assay was determined by rapid filtration through glass-fiber filter strips (Whatman GF/B). The filters were rinsed with 2−4 mL portions of ice-cold Tris-HCl buffer as described above. Radioactivity bound to the filters was quantitated by liquid scintillation spectrometry. Nonspecific binding was determined as binding in the presence of 5 μM diazepam and represented about 10% of total binding.

[^{3}H]PK11195 Binding. The tissues were thawed and homogenized in 50 volumes of Dulbecco's phosphate-buffered saline (PBS; pH 7.4) at 4 °C with a Polytron PT 10 (setting 5, for 20 s). The homogenate was centrifuged at 40000*g* for 30 min, and the pellet was resuspended in 50 volumes of PBS and recentrifuged. The new pellet was resuspended in 20 volumes of PBS and used for the assay. [^{3}H]PK11195 binding was determined in a final volume of 1000 μL of tissue homogenate (0.15−0.20 mg of protein), 100 μL of [^{3}H]PK11195 (specific activity = 85.5 Ci/mmol, New England Nuclear) at a final assay concentration of 1 nM, 5 μL of drug solution or solvent, and 795 μL

Scheme 1 [a]

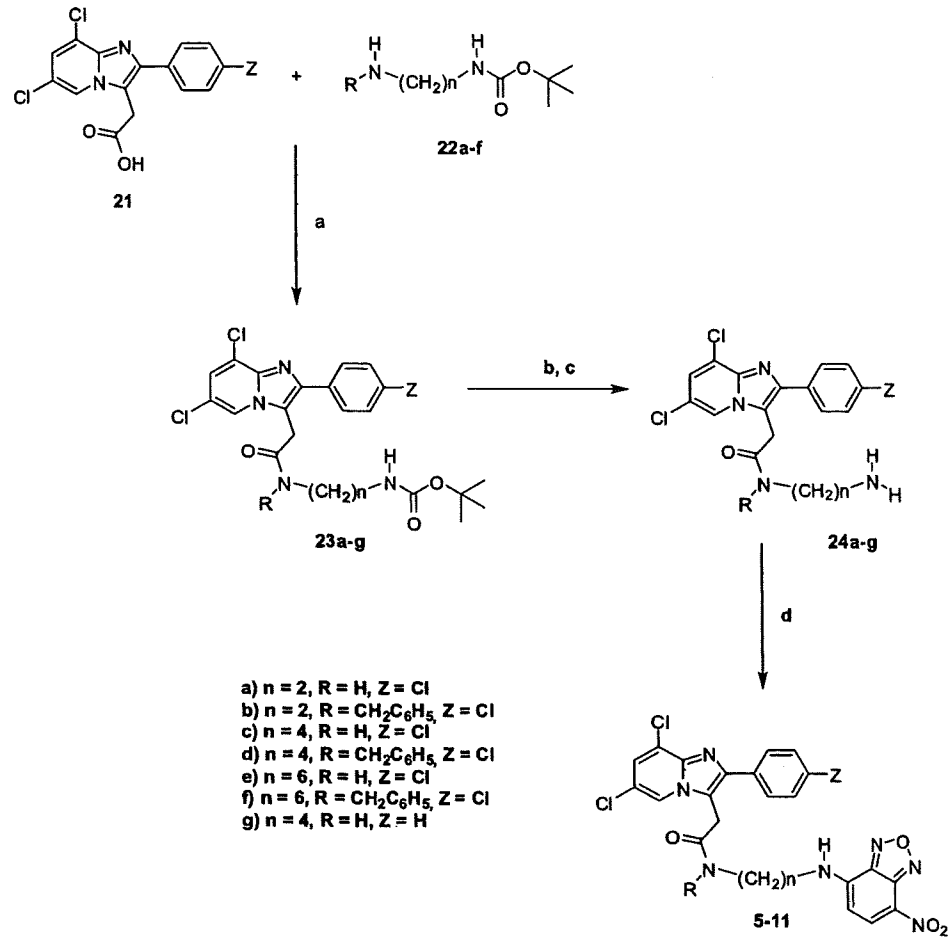

[a] Reagents: (a) THF, TEA, EEDQ; (b) HCl gas, CH_2Cl_2; (c) Na_2CO_3, H_2O; (d) NBD-chloride, THF, TEA.

of PBS buffer (pH 7.4 at 25 °C). Incubations (25 °C) were initiated by the addition of membranes and were terminated 90 min later by rapid filtration through glass-fiber filter strips (Wathaman GF/B), which were rinsed five times with 4 mL of ice-cold PBS buffer using a Cell Harvester filtration manifold (Brandel). Filter-bound radioactivity was quantitated by liquid scintillation spectrometry. Nonspecific binding was defined as binding in the presence of 10 μM unlabeled PK11195 (Sigma-Aldrich, St. Louis, MO).

Cell Cultures. Ra2, an immortalized microglial clone, was established from a mouse primary microglial culture and maintained in Eagle's minimum essential medium (MEM) supplemented with 10% calf serum, 5 μg/mL bovine insulin, 0.2% glucose, and 1 ng/mL recombinant mouse granulocyte-macrophage colony stimulating factor (Genzyme, Cambridge, MA), which is essential for Ra2 growth in culture.

Ra2 cells were seeded at a density of 6500 cells/cm^2 on a glass cover slip and then cultured for 16 h. Compound **10** was added to the Ra2 culture at a final concentration of 1 μM followed by the addition of Mito Tracker Red after 10 min (a dye useful for staining mitochondria in live cells) (Molecular Probes, Eugene, OR) and was then incubated at 37 °C for 1 h. After treatment, Ra2 cells were observed by a fluorescent microscope and photographed. The Ra2 cells were then incubated for 24 h with 1 μg/mL lipopolysaccharide (LPS) (Sigma-Aldrich), which is an endotoxin from *Escherichia coli* and a potent activator of microglia.

In Vivo Biodistribution Study on Compound 10. Adult male C57BL/6 mice were deeply anesthetized with sodium pentobarbital (25 mg/kg, ip) before surgery and remained under anesthesia throughout the entire procedure. When spinal reflexes were absent, a transverse incision was made and then the right carotid artery was exposed and dissected free of surrounding tissues. After the temporary occlusion of proximal site of the carotid artery with an aneurysm clip, a small hole was made in the distal site of the artery with a 27-gauge needle, and a polyethylene tube (Becton Dickinson) was inserted into the proximal site of the artery from the pole. After the aneurysm clip was released, 0.2 mL of compound **10** solution (1 μM in the final concentration) or the same volume of fluorescein isothiocyanate labeled dextran (FITC-dextran) (Sigma-Aldrich, average molecular weight over 250 000; 5 μM in the final concentration) were injected as a bolus over 30 s into the recipient's carotid artery through the polyethylene tube. The solution of compound **10** for injection was obtained from a stock solution (2.9 mM) in dimethyl sulfoxide in turn diluted to 1.0 μM with phosphate-buffered solution (pH 7.2).

Sampling for Fluorescence Observation. At 30 min after injection, animals were additionally anesthetized, and their blood was washed out by transcardial perfusion of isotonic saline solution. Then brains and livers were removed, frozen in liquid nitrogen, and embedded in OTC compound (Tissue Tek, Elkhart, IN). Coronal sections (8 μm) were cut in a cryostat and mounted on slides and dried. Then sections were fixed by 4% paraformaldehyde. Fluorescent observation was performed with a fluorescence microscope (Olympus BX50).

RESULTS AND DISCUSSION

The synthesis of compounds **5**–**11** was accomplished according to the procedure shown in Scheme 1. Synthesis involved the condensation of the suitably substituted imidazopyridineace-

Scheme 2 [a]

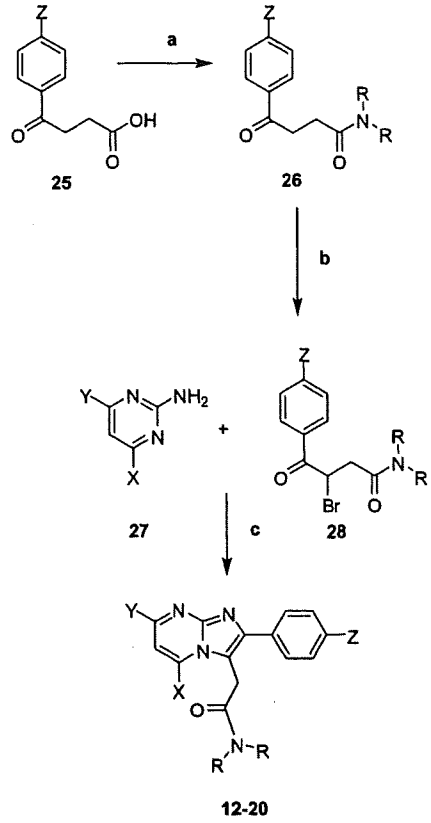

[a] Reagents: (a) R_2NH, TEA, EEDQ, THF; (b) Br_2/CCl_4; (c) DMF reflux.

tic acids **21** (*17*) with the appropriate mono-*N*-Boc-protected diamine compounds **22a–f** (*32*, *33*) in anhydrous THF and in the presence of EEDQ to give the corresponding amides **23a–g**. The Boc deprotection of these last compounds yielded the corresponding compounds **24a–g**, which, in turn, by condensation with 7-nitro-2-oxa-1,3-diazole chloride (NBD-Cl) in anhydrous THF and in the presence of TEA afforded the desired compounds **5–11**. The synthesis of the imidazo[1,2-*a*]pyrimidines **12–20** was carried out as outlined in Scheme 2. Condensation of suitably substituted 2-aminopyrimidine **27** with the appropriate bromoketoamide **28** in refluxing DMF gave compounds **12–20** in moderate to good yield. In principle, by using 2-amino-4-methylpyrimidine in the condensation reaction, two regioisomeric compounds **14** and **14′** or **16** and **16′**, respectively, may be produced. The structural assignment of the isolated compounds is based on the analysis of 2D NOESY ^1H NMR spectra, which showed the presence of cross-peaks between the proton linked at C(5) and the protons of the methylene group at C(3) of the imidazopyrimidine nucleus, being consistent with the **14** and **16** structures only. The starting 2-aminopyrimidine **27** was commercially available, whereas compound **28** was prepared according to a two-step procedure and summarized in Scheme 2 (*28*, *29*). This involved the condensation of the commercially available 3-benzoylpropionic acid **25** with the required dialkylamines in the presence of EEDQ as a dehydrating agent. Treatment of the resulting amide **26** with bromine in carbon tetrachloride afforded compound **28**. All compounds were fully characterized by IR, ^1H NMR, mass spectra, and elemental analyses. The yields and physical data for the final compounds are reported in Table 1.

Radioligand Binding Assays. The affinity of compounds **5–20** for CBR and PBR was assessed by measuring their ability to displace [^3H]flunitrazepam and [^3H]PK11195, respectively, from binding to membrane preparations from the cerebral cortex.

Table 2. Affinity for Rat Cerebrocortical CBR and PBR of Compounds 5–20 and Their Maximum Excitation and Emission Wavelengths

compd	CBR[a] IC_{50} (nM)	PBR[b] (cortex) IC_{50} (nM)	λ_{max} Ex (nm)	λ_{max} Em (nm)
5	(32)	(32)	465	522
6	(39)		465	522
7	(7)	(23)	465	522
8	(18.8)	(38)	465	522
9	(2)	(22)	465	522
10	(1.8)	6700	465	541
11	(15.8)	(18)	465	520
12	>10000	5200	336	350
13	11400	165		
14	9150		240	260
15	10300	82	336	350
16	24000	609	336	350
17		33.7		
18	19670	36	336	350
19	>10000	4700		
20	>10000	6900		
PK11195	24250	1.06		

[a] In parentheses are reported the percentages of [^3H]flunitrazepam inhibition at 10^{-5} M. [b] In parentheses are reported the percentages of [^3H]PK11195 inhibition at 10^{-5} M.

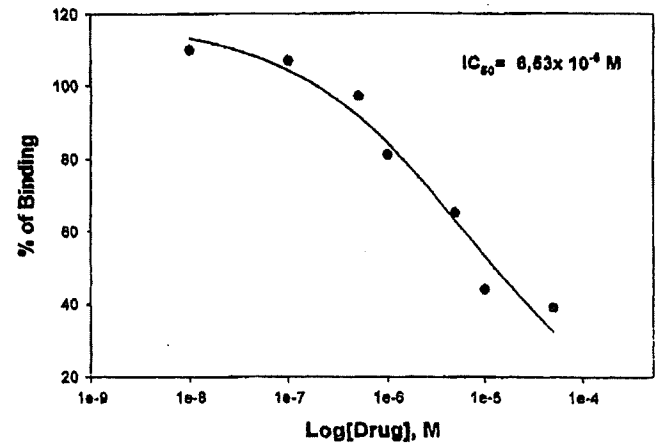

Figure 1. Inhibition of [^3H]PK11195 binding to rat cerebrocortical membranes by compound **10**.

Their effects were compared with those of unlabeled PK11195, and the results of these analyses are shown in Table 2. Compounds **5–11**, including both monoalkyl- and dialkylamides with *n* varying from 2 to 6, generally showed low affinity and selectivity for PBR. However, dialkylamides were more active and selective than monoalkylamides, and significant improvement in affinity and selectivity was observed by increasing the spacer chain length. In this subset of compounds, **10** ($n = 6$, R = $CH_2C_6H_5$) seemed to be the most interesting one, showing an IC_{50} value of 6.7 μM. Figure 1 shows the inhibition of [^3H]-PK11195 binding to rat cerebrocortical membranes by compound **10**. Analysis of the present binding data clearly demonstrates that imidazopyridine PBR ligands linked via a fluorogenic 7-nitro-2,1,3-benzoxadiazol- 4-yl spacer group give rise to new ligands with reduced affinity for the receptor, whereas this was not observed when the same fluorogenic group and spacer were linked to 2-phenylindole-3-acetic acid to give compound **1** (*19*). Thus, for example, compound **8** showed affinity and selectivity for PBR much lower than those of the previously described PBR ligand *N*-benzyl-*N*-*n*-butyl-(2-phenyl-6,8-dichloroimidazo[1,2-*a*]pyridin-3-yl)acetamide (*29*) (i.e., 18% of [^3H]PK11195 inhibition at 10^{-5} M versus IC_{50} 14 nM, respectively).

On the other hand, compounds **12–20** showed different affinities for the PBR ranging from the moderate (i.e., in the

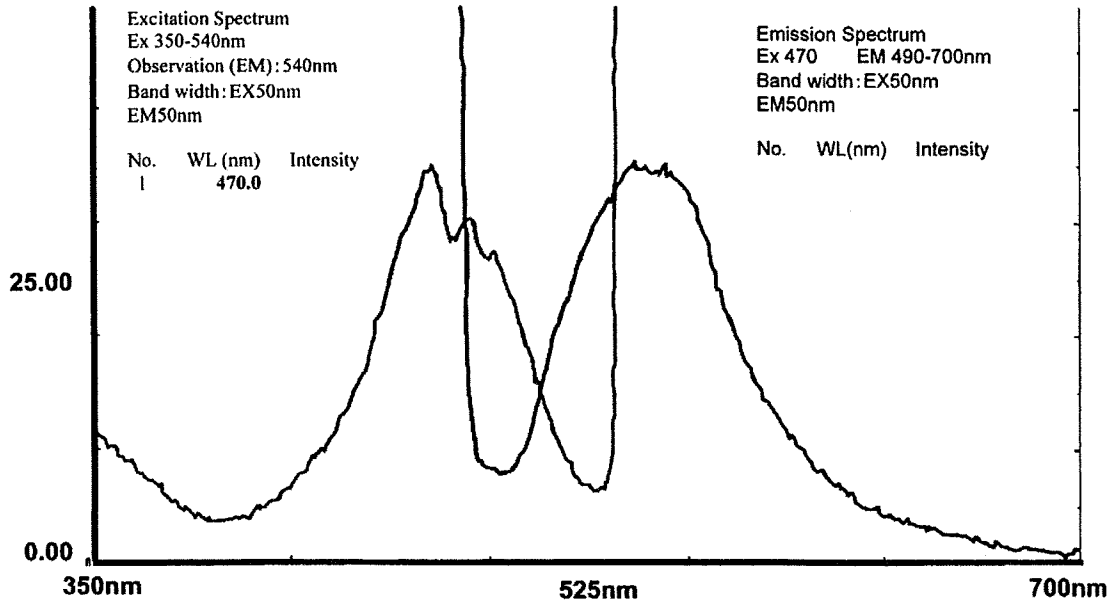

Figure 2. Fluorescence spectrum of compound **10** (excitation at λ 470 and 483 nm) recorded in phosphate-buffered saline (pH 7.2). Compound **10** in dimethyl sulfoxide at 10 mM was diluted to 100 nM in phosphate-buffered saline (pH 7.2) and then the fluorescence spectrum measured by fluorescent spectrophotometer (Shimadzu RF-5300, Shimadzu Co., Kyoto, Japan).

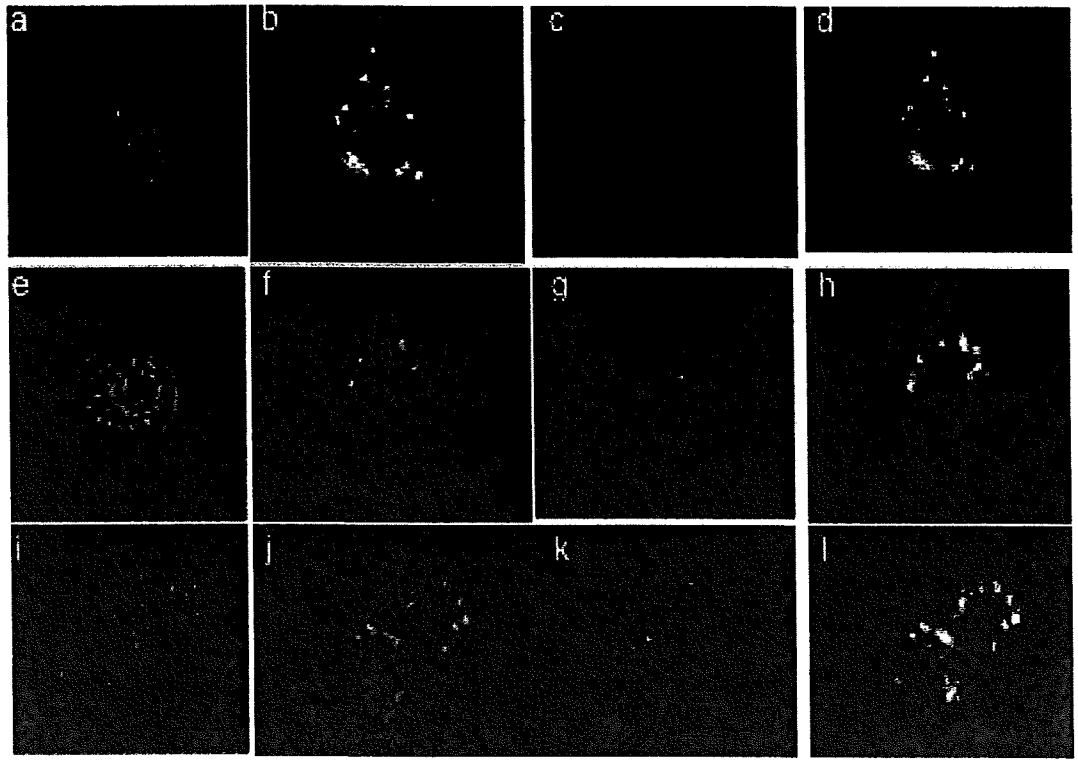

Figure 3. Fluorescent images of Ra2 microglia stimulated with (e–l) or without (a–d) LPS: (a, e, i) phase optics; (b, f, j) fluorescent optics of microglia stained with compound **10**; (c, g, k) fluorescent optics of microglia stained with Mito Tracker Red; (d, h, l) merged optics of fluorescence images of green (compound **10**) and red (Mito Tracker Red).

micromolar range, **12**, **19**, **20**) to high affinity (i.e., in the nanomolar range, **13**, **15**–**18**). Among the compounds of this subset, **17** and **18** were the most active and selective for the PBR, with selectivity indices (defined as the ratio IC_{50} CBR/IC_{50} PBR) of 278 and 546, respectively. From a structure–affinity relationship point of view, it can be pointed out in this subset that alkyl substituents of optimum length on the carboxamide nitrogen and substitution at the para position of the phenyl ring at C(2) of the imidazopyrimidine nucleus with a chlorine atom are crucial for high affinity and selectivity (compare the binding affinities of **15** and **16** as well as **18** and **19**, respectively).

Fluorescence Characteristics of Compounds 5–20. All of the examined compounds **5**–**20** showed a visible fluorescence, and the optimum excitation and emission wavelengths are summarized in Table 2. The data were recorded in methanol as solvent by using a Kontron UV–vis spectrometer and a Perkin-Elmer LS-50B spectrofluorometer. As can be seen from Table 2, the intrinsically fluorescent compounds **12**–**20** exhibited fluorescence emission maxima in the range of 260–350 nm,

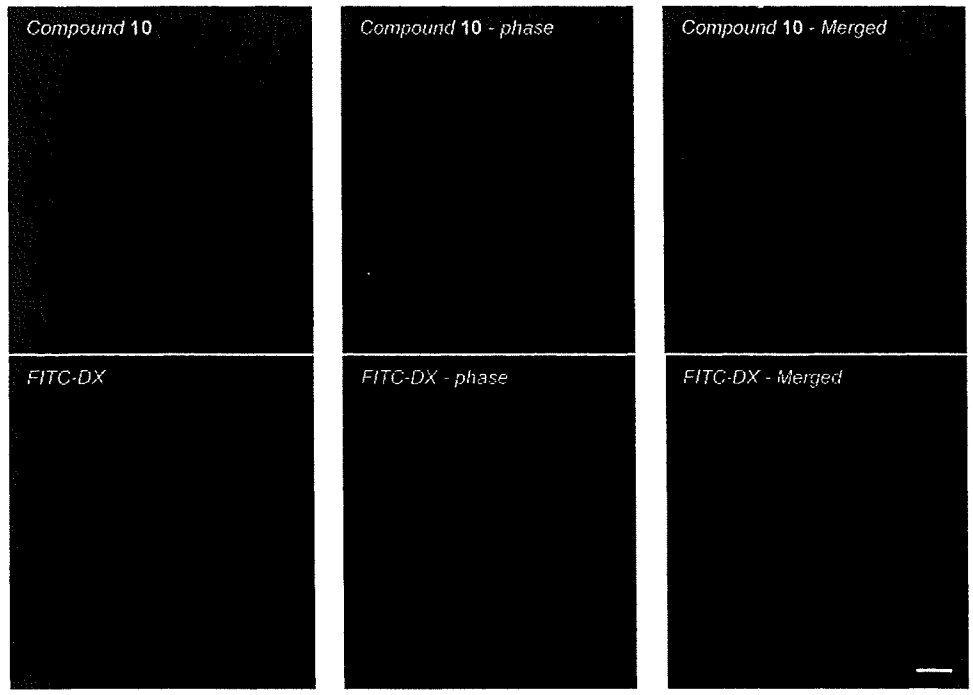

Figure 4. In vivo distribution of compound **10** and FITC-dextran in liver. Liver sections from mouse injected with **10** (upper panels) or FITC-dextran (lower panels) were observed with green fluorescence (left panels) and phase contrast (center panels). Right panels indicate the merged optics of green fluorescence and phase contrast. Bar = 20 μm.

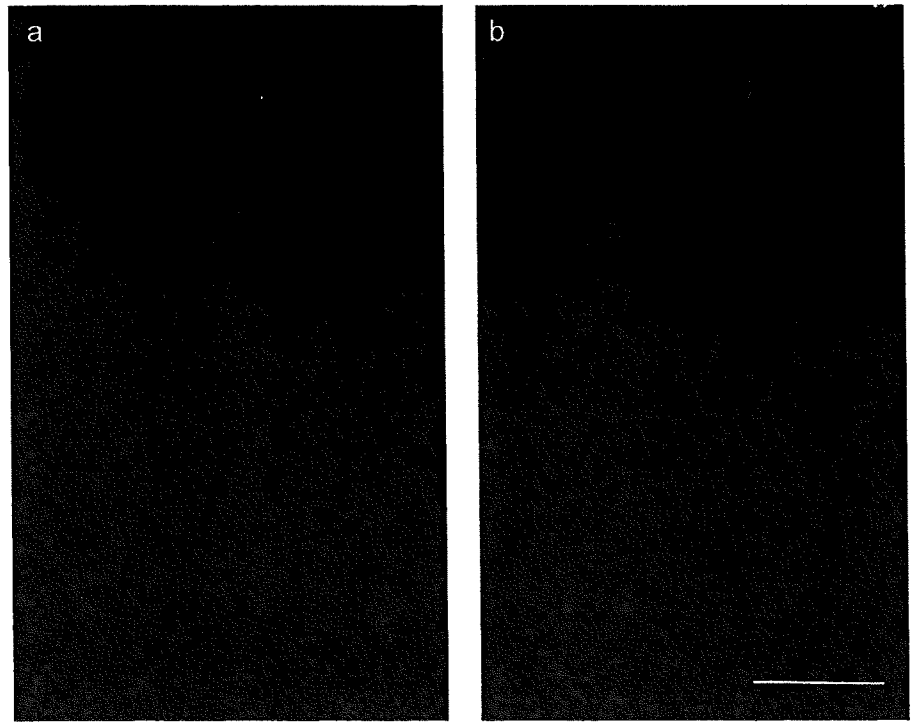

Figure 5. In vivo distribution of compound **10** and FITC-dextran in brain. Brain sections from mouse injected with **10** (a) or FITC-dextran (b) were observed with green fluorescence. Bar = 50 μm.

and thereby their use to successfully visualize PBR is restricted because these wavelengths correspond to those at which many cells and tissues autofluoresce. In contrast, compounds **5**−**11**, bearing the 7-nitrobenzofurazan probe, showed fluorescence emission at longer wavelengths (520−541 nm) and, hence, might be useful for visual imaging of PBR. Thus, in this subset, compound **10** as the most active and selective ligand for PBR was used in fluorescence microscopy studies. Figure 2 shows the fluorescence spectrum of compound **10** with the principal excitation and emission wavelengths at 470, 473, and 541 nm, respectively. Although compound **10** is characterized by a micromolar binding affinity to PBR, literature reports suggest (*21*, *22*) it still can be useful for cellular targeting applications.

Cell Biology, Fluorescence Microscopy, and in Vivo Biodistribution Study on Compound 10. Compound **10** was found to stain live Ra2 microglial cells effectively. Intense fluorescence was observed as a deposit-like pattern mainly distributed in cytosol. Some of the fluorescent deposits were observed to associate with the plasma membrane. Many compound **10**-positive deposits were also stained with Mito Tracker Red, suggesting that compound **10** binding sites may

exist on mitochondria. Large deposits that were not stained with Mito Tracker Red were sometimes observed.

Compound **10**-positive fluorescent deposits were translocated from cytosol to the plasma membrane by LPS stimulation. Some of the deposits were still positive for Mito Tracker Red staining (Figure 3).

The experiments showed that intracellular fluorescent labeling was obtained by using a concentration of 1 μM **10**, that is, a concentration about one-sixth lower than its IC_{50} value.

Compound **10** was used in a biodistribution study to evaluate its utility as a targeting moiety in vivo. Preliminarily, the stability of compound **10** was studied both in 0.05 M phosphate buffer at pH 7.4 and in diluted rat serum solution at 37 °C. Pseudo-first-order kinetics were always observed, and the half-lives were found to be >3 h.

After injection in the carotid artery of adult male C57BL/6 mice of compound **10** and FITC-dextran, used as a control dye, and successive brain and liver removal, it was found that in liver sections compound **10** penetrates to liver parenchyma and stains hepatocytes, whereas FITC-dextran was observed to remain in blood vessels (Figure 4). On the other hand, as for the distribution to brain, the patterns of staining with **10** and FITC-dextran are similar, indicating that both of them hardly penetrate into the brain because of the existence of the blood–brain barrier (BBB) (Figure 5).

In conclusion, some fluorescent imidazopyridine and imidazopyrimidine compounds **5**–**20** were synthesized, and their affinity for PBR was determined. Although members of the subset **12**–**20** possess good PBR binding affinity, they are characterized by a fluoroscence emission wavelength that prevents their use in successfully visualizing PBR. In contrast, compounds **5**–**11** fluoresce at a longer wavelength but possess a low to moderate affinity for PBR. Compound **10** was shown to be the most active derivative and represents a new fluorescent probe for visualization of activated microglia and PBR. It may have some significant advantages (structural simplicity, cost-effective, easy to handle) over the fluorescent or radioactive probes for PBR currently used. In particular, a comparison with compounds **1** [Kozikowski's compound, utilizing the same fluorophore (NBD)] and **3**, both characterized by simple structure and involving no linkages with transition metals, reveals that compound **10** should possess better BBB penetration properties on the basis of its log C_{brain}/C_{blood} (log BB) value (−0.54 compared with −1.06 of **1** and −1.78 of **3**) as estimated by using Clark's model (*34*), which relates log BB to polar surface area. This last descriptor was computed with a fragment-based approach, known as the topological PSA (TPSA) approach (*35*). It is generally accepted that compounds with log BB > 0.3 cross the BBB readily, whereas compounds with log BB < −1.0 are poorly distributed to the brain. On the basis of the predicted log BB values, compound **10** should be able to cross the BBB, whereas compounds **1** and **3** as such should be unable to. The observed in vivo poor BBB penetration of **10** might be due to the possibility that this compound is a substrate of Pglyco efflux protein (Pgp) or to extensive binding to serum proteins. From the results of cell culture and in vivo injection, it can be stated that compound **10** is a new useful tool of bioimaging for PBR and has potential to generate new information on the pathological role of this receptor in vivo. Further studies are in progress to synthesize additional compounds, particularly those that combine high affinity and selectivity for PBR and fluorescence emission at long wavelengths as well as good BBB penetration properties.

ACKNOWLEDGMENT

This work was supported by a grant from Ministero dell'Istruzione dell'Università e dellaRicerca (COFIN 2004 MIUR to G.T.). We thank Giovanni Dipinto for skillful technical assistance in recording mass spectra and determining microanalytical data. We also thank Dr. Kelly Desino (The University of Kansas) for helpful discussion.

LITERATURE CITED

(1) Anholt, R. R. H., Pedersen, P. L., De Souza, E. B., and Snyder, S. H. (1986) The peripheral benzodiazepine receptor: localization to the mitochondrial outer membrane. *J. Biol. Chem. 261*, 576–583.

(2) Papadopoulos, V., Baraldi, M., Guilarte, T. R., Knudsen, T. B., Lacapere, J. J., Lindemann, P., Norenberg, M. D., Nutt, D., Weizman, A., Zhang, M. R., and Gavish, M. (2006) Translocator protein (18 kDa): new nomenclature for the peripheral-type benzodiazepine receptor based on its structure and molecular function. *Trends Pharmacol. Sci. 27*, 402–409.

(3) Papadopulos, V., Guarneri, P., Krueger, K. E., Guidotti, A., and Costa, E. (1992) Pregnenolone biosynthesis in C6 glioma cell mitochondria: regulation by a mitochondrial diazepam binding inhibitor receptor. *Proc. Natl. Acad. Sci. U.S.A. 89*, 5113–5117.

(4) Messmer, K., and Reynolds, G. P. (1998) Increased peripheral benzodiazepine binding site in the brain of patients with Huntington's disease. *Neurosci. Lett. 241*, 53–56.

(5) Veenman, L., and Gavish, M. (2000) Peripheral-type benzodiazepine receptors: their implication in brain disease. *Drug Dev. Res. 50*, 355–370.

(6) Benveniste, E. N. (1997) Role of macrophages/microglia in multiple sclerosis and experimental allergic encephalomyelitis. *J. Mol. Med. 75*, 165–173.

(7) Cagnin, A., Brooks, D. J., Kennedy, A. M., Gunn, R. N., Myers, R., and Turkheimer, F. E. (2001) In-vivo measurement of activated microglia in dementia. *Lancet 358*, 461–467.

(8) Kassiou, M., Meikle, S. R., and Banati, R. B. (2005) Ligands for peripheral benzodiazepine binding sites in glial cells. *Brain Res. Rev. 48*, 207–210.

(9) Hardwick, M., Fertikh, D., Culty, M., Li, H., Vidic, B., and Papadopoulos, V. (1999) Peripheral-type benzodiazepine receptor (PBR) in human breast cancer: correlation of breast cancer cell aggressive phenotype with PBR expression, nuclear localization, and PBR-mediated cell proliferation and nuclear transport of cholesterol. *Cancer Res. 59*, 831–842.

(10) Katz, Y., Eitan, A., and Gavish, M. (1990) Increased density of peripheral benzodiazepine binding sites in ovarian carcinomas as compared with benign ovarian tumors and normal ovaries. *Clin. Sci. 78*, 155–158.

(11) Venturini, I., Zaneroli, M. L., Corsi, L., Avallona, R., Farina, F., Alho, H., Baraldi, C., Ferrarese, C., Pecora, N., Frigo, M., Ardizzone, G., Arrigo, A., Pellicci, R., and Baraldi, M. (1998) Up-regulation of peripheral benzodiazepine receptor system in hepatocellular carcinoma. *Life Sci. 65*, 1269–1280.

(12) Hirsch, T., Decaudin, D., Susin, S. A., Marchetti, P., Larochette, N., Resche-Rigon, M., and Kroemer, G. (1998) PK 11195, a ligand of the mitochondrial benzodiazepine receptor, facilitates the induction of apoptosis and reverses Bcl-2 mediated cytoprotection. *Exp. Cell Res. 241*, 426–34.

(13) Sutter, A. P., Maaser, K., Barthel, B., and Scherübl, H. (2003) Ligands of the peripheral benzodiazepine receptor induce apoptosis and cell cycle arrest in oesophageal cancer cells: involvement of the p38mapk signalling pathway. *Br. J. Cancer 89*, 564–572.

(14) Xia, W., Spector, S., Hardy, L., Zhao, S., Saluk, A., Alemane, L., and Spector, N. L. (2000) Tumor selective G2/M cell cycle arrest and apoptosis of epithelial and hematological malignancies by BBL22, a benzazepine. *Proc. Natl. Acad. Sci. U.S.A. 97*, 7494–7499.

(15) Galiegue, S., Tinel, N., and Casellas, P. (2003) The peripheral benzodiazepine receptors: a promising therapeutic drug target. *Curr. Med. Chem. 10*, 1563–1572.

(16) Kupczyk-Subotkowaka, L., Siahaan, T. J., Basile, A., Friedman, H. S., Higgins, P. E., Song, D., and Gallo, J. M. (1997) Modulation of melphalan resistance in glioma cells with a peripheral benzodiazepine receptor ligand–melphalan conjugate. *J. Med. Chem. 40*, 1726–1730.

(17) Trapani, G., Laquintana, V., Latrofa, A., Ma, J., Reed, K., Serra, M., Biggio, G., Liso, G., and Gallo, J. M. (2003) Peripheral

benzodiazepine receptor ligand−melphalan conjugates for potential selective drug delivery to brain tumors. *Bioconjugate Chem. 14*, 830−839.

(18) Guo, P., Ma, J., Li, S., Guo, Z., Adams, A. L., and Gallo, J. M. (2001) Targeted delivery of a peripheral benzodiazepine receptor ligand−gemcitabine conjugate to brain tumors in a xenograft model. *Cancer Chemother. Pharmacol. 48*, 169−176.

(19) Kozikowski, A. P., Kotoula, M., Ma, D., Boujrad, N., Tuckmantel, W., and Papadopoulos, V. (1997) Synthesis and biology of a 7-nitro-2,1,3-benzoxadiazol-4-yl derivative of 2-phenylindole-3-acetamide: a fluorescent probe for the peripheral-type benzodiazepine receptor. *J. Med. Chem. 40*, 2435−2439.

(20) Manning, H. C., Goebel, T., Thompson, R. C., Price, R. R., Lee, H., and Bornhop, D. J. (2004) Targeted molecular imaging agents for cellular-scale bimodal imaging. *Bioconjugate Chem. 15*, 1488−1495.

(21) Manning, H. C., Smith, S. M., Sexton, M., Haviland, S., Bai, M., Cederquist, K., Stella, N., and Bornhop, D. J. (2006) A peripheral benzodiazepine receptor targeted agent for in vitro imaging and screening. *Bioconjugate Chem. 17*, 735−740.

(22) Chen, Y., Zheng, X., Dobhal, M. P., Gryshuk, A., Morgan, J., Dougherty, T. J., Oseroff, A., and Pandey, R. K. (2005) Methyl pyrophorbide-α analogues: potential fluorescent probes for the peripheral-type benzodiazepine receptor. Effect of central metal in photosensitizing efficacy. *J. Med. Chem. 48*, 3692−3695.

(23) Romeo, E., Auta, J., Kozikowski, A. P., Ma, A., Papadopoulos, V., Puia, G., Costa, E., and Guidotti, A. (1992) 2-Aryl-3-indoleacetamides (FGIN-1): a new class of potent and specific ligands for the mitochondrial DBI receptor. *J. Pharmacol. Exp. Ther. 262*, 971−978.

(24) Le Fur, G., Perrier, M. L., Vaucher, N., Imbault, F., Flamier, A., Uzan, A., Renault, C., Dubroeucq, M. C., and Gueremy, C. (1983) Peripheral benzodiazepine binding sites: effect of PK11195, 1-(2-chlorophenyl)-*n*-(1-methylpropyl)-3-isoquinolinecarboxamide I. In vitro studies. *Life Sci. 32*, 1839−1847.

(25) Marangos, P. L., Pate, J., Boulenger, J. P., and Clark-Rosenberg, R. (1982) Characterization of peripheral-type benzodiazepine binding sites in brain using [3H]Ro 5-4864. *Mol. Pharmacol. 22*, 26−32.

(26) Okujama, S., Chaki, S., Yoshikawa, R., Ogawa, S., Suzuki, Y., Okubo, T., Nakazato, A., Nagamine, M., and Tomisawa, K. (1999) Neuropharmacological profile of peripheral benzodiazepine receptor agonists, DAA1097 and DAA1106. *Life Sci. 16*, 1455−1464.

(27) Trapani, G., Franco, M., Ricciardi, L., Latrofa, A., Genchi, G., Sanna, E., Tuveri, F., Cagetti, E., Biggio, and Liso, G. (1997) Synthesis and binding affinity of 2-phenyl-imidazo[1,2-*a*]pyridine derivatives for both central and peripheral benzodiazepine receptors. A new series of high-affinity and selective ligands for the peripheral type. *J. Med. Chem. 40*, 3109−3118.

(28) Trapani, G., Franco, M., Latrofa, A., Ricciardi, L., Carotti, A., Serra, M., Sanna, E., Biggio, G., and Liso, G. (1999) Novel 2-phenylimidazo[1,2-*a*]pyridine derivatives as potent and selective ligands for peripheral benzodiazepine receptors. synthesis, binding affinity, and *in vivo* studies. *J. Med. Chem. 42*, 3934−3941.

(29) Trapani, G., Laquintana, V., Denora, N., Trapani, A., Lopedota, A., Latrofa, A., Franco, M., Serra, M., Pisu, M. G., Floris, I., Sanna, E., Biggio, G., and Liso, G. (2005) Structure−activity relationships and effects on neuroactive steroids in a series of 2-phenylimidazo-[1,2-*a*]pyridineacetamide peripheral benzodiazepine receptors ligands. *J. Med. Chem. 48*, 292−305.

(30) Rackham, D. M. (1979) Spectroscopic studies of some imidazo-[1,2-*a*]pyridine and imidazo[1,2-*a*]pyrimidine derivatives. *Appl. Spectrosc. 33*, 561−563.

(31) Janssen, M. J., Ensing, K., and De Zeew, R. A. (2000) Fluorescent-labeled ligands for the benzodiazepine receptor. *Pharmazie 55*, 102−106.

(32) Muller, D., Zeltser, I., Bitan, G., and Gilon, C. (1997) Building units for N-backbone cyclic peptides. 3. Synthesis of protected N^{α}-(ω-aminoalkyl)amino acids and N^{α}-(ω-carboxyalkyl)amino acids. *J. Org. Chem. 62*, 411−416.

(33) Martin, B., Possémé, F., Le Barbier, C., Careaux, F., Carboni, B., Seiler, N., Moulinoux, J.-P., and Delcros, J.-G. (2001) *N*-Benzylpolyamines as vectors of boron and fluorine for cancer therapy and imaging: synthesis and biological evaluation. *J. Med Chem. 44*, 3653−3664.

(34) Clark, D. E. (1999) Rapid calculation of polar molecular surface area and its application to the prediction of transport phenomena. 2. Prediction of blood−brain barrier penetration. *J. Pharm. Sci. 88*, 815−821.

(35) Ertl, P., Rohde, B., and Selzer, P. (2000) Fast calculation of molecular polar surface area as a sum of fragment-based contributions and its application to the prediction of drug transport properties. *J. Med. Chem. 43*, 3714−3717.

BC060393C

2007

J Neural Transm (2007) [Suppl 72]: 113–120

Printed in Austria

Journal of Neural Transmission

Biochemistry of postmortem brains in Parkinson's disease: historical overview and future prospects

T. Nagatsu[1,2], M. Sawada[1]

[1] Department of Brain Life Science, Research Institute of Environmental Medicine, Nagoya University, Nagoya, Aichi, Japan
[2] Department of Pharmacology, School of Medicine, Fujita Health University, Toyoake, Aichi, Japan

Summary Biochemical studies on postmortem brains of patients with Parkinson's disease (PD) have greatly contributed to our understanding of the molecular pathogenesis of this disease. The discovery by 1960 of a dopamine deficiency in the nigro-striatal dopamine region of the PD brain was a landmark in research on PD. At that time we collaborated with Hirotaro Narabayashi and his colleagues in Japan and with Peter Riederer in Germany on the biochemistry of PD by using postmortem brain samples in their brain banks. We found that the activity, mRNA level, and protein content of tyrosine hydroxylase (TH), as well as the levels of the tetrahydrobiopterin (BH4) cofactor of TH and the activity of the BH4-synthesizing enzyme, GTP cyclohydrolase I (GCH1), were markedly decreased in the substantia nigra and striatum in the PD brain. In contrast, the molecular activity (enzyme activity/enzyme protein) of TH was increased, suggesting a compensatory increase in the enzyme activity. The mRNA levels of all four isoforms of human TH (hTH1–hTH4), produced by alternative mRNA splicing, were also markedly decreased. This finding is in contrast to a completely parallel decrease in the activity and protein content of dopamine β-hydroxylase (DBH) without changes in its molecular activity in cerebrospinal fluid (CSF) in PD. We also found that the activities and/or the levels of the mRNA and protein of aromatic L-amino acid decarboxylase (AADC, DOPA decarboxylase), DBH, phenylethanolamine N-methyltransferase (PNMT), which synthesize dopamine, noradrenaline, and adrenaline, respectively, were also decreased in PD brains, indicating that all catecholamine systems were widely impaired in PD brains. Programmed cell death of the nigro-striatal dopamine neurons in PD has been suggested from the following findings on postmortem brains: (1) increased levels of pro-inflammatory cytokines such as TNF-α and IL-6; (2) increased levels of apoptosis-related factors such as TNF-α receptor R1 (p 55), soluble Fas and bcl-2, and increased activities of caspases 1 and 3; and (3) decreased levels of neurotrophins such as brain-derived nerve growth factor (BDNF). Immunohistochemical data and the mRNA levels of the above molecules in PD brains supported these biochemical data. We confirmed by double immunofluorescence staining the production of TNF-α and IL-6 in activated microglia in the putamen of PD patients. Owing to the recent development of highly sensitive and wide-range analytical methods for quantifying mRNAs and proteins, future assays of the levels of various mRNAs and proteins not only in micro-dissected brain tissues containing neurons and glial cells, but also in single cells from frozen brain slices isolated by laser capture micro-dissection, coupled with toluidine blue, Nissl staining or immunohistochemical staining, should further contribute to the elucidation of the molecular pathogenesis of PD and other neurodegenerative or neuropsychiatric diseases.

Keywords: Parkinson's disease, postmortem brain, laser micro-dissection, biochemistry, enzymes, cytokines, neurotrophins

Correspondence: Prof. Dr. Toshiharu Nagatsu, Department of Pharmacology, Fujita Health University, Toyoake, Aichi, Japan
e-mail: tnagatsu@fujita-hu.ac.jp

Introduction

The main symptoms of movement disorder, i.e., akinesia, muscle rigidity, and resting tremor, in Parkinson's disease (PD) are caused by a deficiency in the level of the neurotransmitter dopamine at the nerve terminals in the striatum of the nigro-striatal dopamine neurons as the result of selective neurodegeneration of dopamine neurons in the substantia nigra. Most PD is aging-related and sporadic without any hereditary history. Familial PD (PARK) is estimated to represent only ~5% of PD cases. The presence of intracelluar inclusions called Lewy bodies, which are mainly composed of α-synuclein (*α-synuclein* is the causative gene of PARK1), is another feature of sporadic PD. The molecular mechanism of neural degeneration in sporadic PD is speculated to be multiple (Riederer et al., 2001; Nagatsu and Sawada, 2006), involving environmental and/or endogenous potential neurotoxins, oxidative stress, mitochondrial dysfunction, altered iron homeostasis, immune-mediated mechanisms, and susceptibility genes that might be related to the causative genes in familial PD (Mizuno et al., 2006) such as *α-synuclein* or *parkin*. Noradrenaline deficiency in noradrenaline neurons is also observed in the locus coeruleus. These dopamine and noradrenaline deficiencies in the brain of PD patients were first observed by Ehringer and Hornykiewicz (1960). As Foley et al. (2000)

pointed out, Sano et al. (1960, 2000) also observed greatly reduced dopamine levels in the substantia nigra and striatum in one case of postmortem PD brain. This discovery of a dopamine deficiency in the nigro-striatum was a landmark finding of biochemical studies on PD, and led to the development of L-DOPA therapy to supplement the deficient dopamine. L-DOPA was the first neurotransmitter supplementation therapy, and it is still the gold standard of drug therapy for PD.

Up to 1960, even after development of sensitive spectrofluorometric assays, biochemical studies on such unstable compounds as dopamine and noradrenaline had been thought to be difficult to conduct on human postmortem brains. However, after the successful confirmation of the dopamine deficiency in the nigro-striatal region in postmortem PD brains in 1960, biochemical studies on postmortem brains were expanded from various small molecules such as catecholamine neurotransmitters to mRNAs and proteins of enzymes and cytokines related to PD, Alzheimer's diseases (AD), and other neurodegenerative or neuropsychiatric diseases, and have greatly contributed to elucidation of their molecular pathogenesis. This review focuses on the historical development and future prospects of biochemical studies on postmortem brains from PD patients.

Problems in the biochemistry of postmortem brain samples

Biochemical quantitative analyses of human postmortem brain samples have intricate problems, because there are many uncontrollable factors in such samples. The following considerations are generally required in biochemical studies using postmortem brain tissues. (1) Approval of the local ethics committee is essential. (2) Precise clinical information on the patient is required, as drugs administered to the patient may affect primarily or secondarily the level of the compound to be assayed. Most PD patients are administered L-DOPA or dopamine receptor agonists. (3) The condition before death such as the cause of death and the duration of coma may affect the objective compound. No consuming diseases and a short agony stage are necessary conditions to obtain reliable biochemical data. (4) Postmortem time may affect the results. Such compounds as dopamine or noradrenaline are unstable and easily degraded non-enzymatically or enzymatically by monoamine oxidase (MAO). mRNAs and proteins are also unstable. Therefore, the postmortem delay must be as short as possible (preferably within 12 h). (5) Age and postmortem time of PD patients must be similar to those of the control patients. (6) The brain regions to be dissected and the methods of brain dissection should be the same between PD brains and control ones. Punching-out of the micro brain regions from tissue slices (~1–2 cm) is generally used, and the brain location to be dissected out must be the same in each brain sample. As described below, single cell analysis by laser micro-dissection (Hashida et al., 2002; Kawahara et al., 2003) will be a new and valuable method to further our knowledge of the biochemistry of the postmortem brain. (7) Dissected samples should be frozen immediately on dry ice, completely packed and sealed, and stocked at −80° in a deep freezer. (8) Since large numbers of samples are required for proper statistical analysis, a brain bank should be established.

Figure 1 shows schematically the brain bank system in Germany (Riederer P, personal communication).

Changes in catecholamine neurotransmitters and related enzymes in postmortem PD brains

After the discovery of the dopamine deficiency in the nigro-striatum in PD, various neurotransmitters and their related enzymes were measured in postmortem PD brains by us and by other workers. Nagatsu's group first collaborated with Hirotaro Narabayashi (Juntendo University School of Medicine, Tokyo, Japan), who supplied the brain samples from his own brain bank (established by Hirotaro Narabayashi and Reiji Iizuka), and further collaborated with Peter Riederer who established a brain bank at Würzburg University (Würzburg, Germany; Fig. 1).

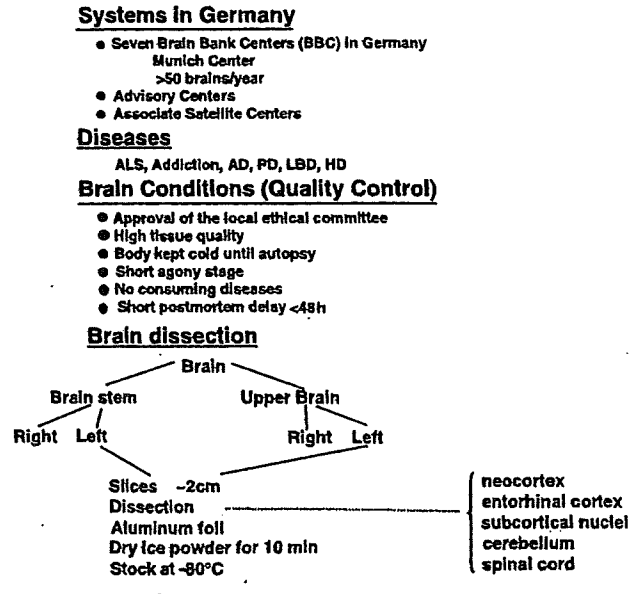

Fig. 1. The brain bank system in Germany (P. Riederer, personal communication)

Table 1. *Changes reported in catecholamine-related enzymes in Parkinson's disease*

Enzymes	Sample source	mRNA	Protein	Activity	Molecular activity (activity/protein)
TH					
Total	striatum		decreased	decreased	increased
Total	SN	decreased	decreased	decreased	increased
hTH1	SN	decreased			
hTH2	SN	decreased			
hTH3	SN	decreased			
hTH4	SN	decreased			
AADC	SN	decreased		decreased	
DBH	CSF		decreased	decreased	normal
	hypothalamus			decreased	
GCH1	striatum			decreased	
PNMT	hypothalamus			decreased	

AADC, aromatic L-amino acid decarboxylase; *CSF*, cerebrospinal fluid; *DBH*, dopamine β-hydroxylase; *GCH1*, GTP cyclohydrolase I; *LC*, locus coeruleus; *PNMT*, phenylethanolamine N-methyltransferase; *SN*, substantia nigra; *TH*, tyrosine hydroxylase.
From Nagatsu et al. (1977, 1981, 1984, 1986), Mogi et al. (1988a, b) and Ichinose et al. (1994).

The results are summarized in Table 1. In our early studies we measured the activities and protein contents of the enzymes related to catecholamine metabolism. We found the presence of phenylethanolamine N-methyltransferase (PNMT) in the control and PD brains, supporting the presence of adrenaline neurons in the human brain (Nagatsu et al., 1977; Trocewicz et al., 1982). We (Nagatsu et al., 1977, 1984) also found a marked decrease (to ~10–20% of controls) in the activity of tyrosine hydroxylase (TH) in the nigro-striatum in PD, in agreement with the results of other workers (Lloyd et al., 1975; McGeer and McGeer, 1976). Riederer et al. (1978) found TH activity to be decreased also in the adrenal medulla in PD, indicating the general impairment of the catecholamine system. DOPA decarboxylase (aromatic L-amino acid decarboxylase, AADC) activity was found to be decreased in the nigro-striatum in PD (Lloyd and Hornykiewicz, 1970). We also found decreased activities in dopamine β-hydroxylase (DBH) for noradrenaline synthesis and PNMT for adrenaline synthesis in PD brains (Nagatsu et al., 1977, 1984). Furthermore, the level of the tetrahydrobiopterin (BH4) cofactor of TH and the activity of the BH4-synthesizing enzyme GTP cyclohydrolase I (GCH1) were found to be decreased in PD brains (Nagatsu et al., 1981, 1986). These results indicate that not only the nigro-striatal dopamine neurons but also all catecholamine neurons are generally affected in PD. Braak et al. (2006) recently proposed, based on the pathology of Lewy bodies, that PD may start in the pre-symptomatic phase from the medulla oblongata where noradrenaline and adrenaline neurons are localized.

The activity of the serotonin-synthesizing enzyme tryptophan hydroxylase (TPH2) was also moderately decreased in the substantia nigra in PD (Sawada et al., 1985). In contrast to PD, in Alzheimer's disease (AD) the activities of TPH2 and TH, and the contents of the biopterin cofactor in the AD brain were found to be moderately decreased in various brain regions, indicating a reduction in the numbers of both serotonin and catecholamine neurons in wide monoamine regions in AD (Sawada et al., 1987).

We examined not only the enzyme activity, but also the protein content measured by enzyme immunoassay, of TH in PD brains. Although both TH protein and TH activity in the nigro-striatum were markedly decreased in parallel in PD brains as compared with those of the control brains, the molecular activity (activity per enzyme protein, also called homo-specific activity) was significantly increased in PD brains. The increase in the molecular activity of residual TH in PD brains suggests that such molecular changes in TH molecules represent a compensatory increase in TH activity (Mogi et al., 1988a). We also measured in cerebrospinal fluid (CSF) of control and PD patients the protein contents and activities of DBH, which synthesizes noradrenaline and adrenaline and is secreted from noradrenaline and adrenaline neurons in the brain into the CSF. In contrast to TH, both DBH activity and protein content in the CSF of PD patients were reduced in parallel ($r=0.79$) to ~20% of control values without changes in the molecular activity, suggesting only a decreased content in DBH without molecular changes in DBH protein in the noradrenaline and adrenaline neurons in PD (Mogi et al., 1988b). Human TH is markedly activated by the cofactor Fe^{2+}. There are no significant changes in the stimulation of TH activity in the human caudate nucleus by Fe^{2+} in PD, whereas such differences are noted between PD and control brains when exogenous protein kinase is used as a stimulant (Rausch et al., 1988).

Four isoform proteins of human TH (hTH1–hTH4) are expressed by alternative mRNA splicing from a single gene in the brain (Haycock, 2002; Grima et al., 1987; Kaneda et al., 1987; Kobayashi et al., 1988). In human AADC, a single protein is produced by a tissue-specific alternative promoter from neuronal and non-neuronal mRNAs encoded by a single gene (Ichinose et al., 1992). We quantified all four types of human TH mRNAs and AADC mRNA in human brains (substantia nigra) from control, PD, and schizophrenia patients by using the quantitative reverse transcription-polymerase chain reaction (RT-PCR;

Ichinose et al., 1994). All four types of TH mRNAs were detected in the substantia nigra in the control brains examined; and the ratio of hTH1, hTH2, hTH3, and hTH4 mRNAs to the total amount of TH mRNAs was 45, 52, 1.4, and 2.1%, respectively, in the substantia nigra. The levels of TH and AADC mRNAs were highly correlated in the control cases. We found that PD brains had very low levels of all four TH isoform mRNAs and AADC mRNA in the substantia nigra compared with control brains, whereas no significant differences were found between schizophrenic brains and normal ones. We found that monkeys [Japanese monkeys (*Macaca irus* and *Macaca fuscata*), gibbon, orangutan, gorilla, and chimpanzee] have two TH isoforms corresponding to hTH1 and hTH2 (Ichikawa et al., 1990; Ichinose et al., 1993). Monkeys, like humans, are highly susceptible to 1-methyl-4-phenyl-1, 2, 3, 6-tetrahydropyridine (MPTP), a chemical that produces PD in humans (Langston et al., 1983). Thus, we also measured the levels of the two types of TH mRNAs in PD monkeys produced by use of MPTP and compared these levels with those for normal monkeys (Ohye et al., 1995). The levels of both monkey TH mRNAs were significantly decreased specifically in the substantia nigra, which results are similar to those in human PD. All these results indicate that catacholamine-synthesizing enzyme systems are generally decreased in all catecholamine neurons especially in the nigro-striatal dopamine neurons. These decreases may be caused by neuronal degeneration. However, it is not still clear yet when such changes in catecholamine-synthesizing enzymes start in catecholamine neurons in relation to neurodegeneration in sporadic PD. We found that in MPTP-produced animal PD models the changes in the TH system occur soon after MPTP treatment, as evidenced first by a decrease in TH activity, then inactivation followed by a decrease in the protein levels (Nagatsu, 1990).

Presence of MPTP-like neurotoxins in postmortem brains in PD

MPTP inhibits complex I in mitochondria, produces reactive oxygen species, and causes apoptotic cell death in MPTP-induced PD in animals. Dopamine cell death in sporadic PD is also thought to be caused by apoptosis (Hirsch et al., 1999). Since MPTP is a chemically synthesized PD-producing neurotoxin in humans, efforts have been made to find MPTP-like neurotoxins in postmortem PD brains by us and by other workers (Nagatsu et al., 1997, 2002a). Two groups of MPTP-like compounds, isoquinolines (IQs) and β-carbolines, were identified in postmortem human PD brain and in CSF by gas chromatography-mass spectrometry. Similar to MPTP, these IQs and β-carbolines generally inhibit mitochondrial complex I, and cause apoptotic death of catecholamine-producing cells in cultures. Like MPTP, which is converted to toxic 1-methyl-4-phenyl-pyridinium (MPP+) by MAO B, IQs and β-carbolines are also generally N-methylated by N-methyltransferase and then oxidized by MAO B to isoquinolinium ions or carbolinium ions to produce neurotoxicity in animals *in vivo*. Some probable neurotoxins such as (R)-N-Me-salsolinol are assumed to be endogenously synthesized from dopamine in the brain. When (R)-N-Me-salsolinol is administered directly into the striatum in rats, it produces Parkinson-like movement disorders (Naoi et al., 1996). These properties are similar to those of MPP+. The following IQs have been identified in the brain of patients with PD and also of control patients (Nagatsu, 1997; 2002a): tetrahydroisoquinoline (TIQ), 1-Me-TIQ, N-Me-TIQ, N-Me-6,7-(OH)2-TIQ (N-Me-norsalsolinol), 1, N-(Me)2-6,7-(OH)2-TIQ (N-Me-salsolinol), 1-phenyl-TIQ, N-Me-1-phenyl-TIQ, and 1-benzyl-TIQ (1-Bn-TIQ). Among these IQ compounds, 1-Bn-TIQ (Kotake et al., 1995) and (R)-N-methyl-salsolinol (Naoi et al., 1996) are the most potent in producing PD in animals. Among β-carbolines, norharman, harman, 2-Me-norharmanium, and 2,9- (Me)2-norharmanium have been identified in the brain and CSF in normal controls and PD (Collins and Neafsey, 2000; Matsubara, 2000). 1-Trichloromethyl-1,2,3,4-tetrahydro-β-carboline (TaClo) is another neurotoxic β-carboline (Bringmann et al., 2000). Some of these neurotoxins are increased in the brain and/or CSF in PD. However, their distributions in the brain are not specific to the nigrostriatal pathway, and none of them, except MPTP, have been proved to produce PD in humans. Therefore, the significance of these neurotoxins with respect to PD remains unknown.

Changes in cytokines and neurotrophins in postmortem brains in PD

The brain is generally considered to be a "privileged" site, i.e., one free from immune reactions, since it is protected by being behind the blood-brain barrier. However, recent findings revealed that immune responses do, in fact, occur in the brain in PD or in other neurodegenerative diseases, probably by microglia activation that produces pro-inflammatory cytokines (Hayley and Anisman, 2005; Hirsch et al., 2003; McGeer and McGeer, 1995; McGeer et al., 1988; Nagatsu and Sawada, 2005; Nagatsu et al., 1999; Sawada et al., 2006). As described below, PD animals produced by

Table 2. *Changes reported in various cytokines, growth factors, and apoptosis-related factors in Parkinson's disease*

Cytokines, growth factors, or apoptosis-related factors	Tissue studied			
	Substantia nigra	Striatum	Ventricular CSF	Lumbar CSF
TNF-α		increased		increased
IL-1β		increased	increased	increased
IL-2		increased	increased	
IL-4			increased	
IL-6		increased	increased	increased
EGF		increased		
TGF-α		increased	increased	
TGF-β1		increased	increased	
TGF-β2			increased	
NGF	decreased			
BDNF	decreased			
GDNF	no change			
bFGF		no change		
TNF R1 (p55)	increased			
caspase 1 (activity)	increased			
caspase 3 (activity)	increased			
β2-microglobulin		increased		
bcl-2		increased		
solubles Fas		increased		

From Nagatsu et al. (1999) and Nagatsu (2002).

MPTP or 6-hydroxydopamine showed apoptotic death of the nigro-striatal dopamine neurons with increased levels of pro-inflammatory cytokines and decreased levels of neurotrophins. Therefore, we examined changes in the levels of pro-apoptotic cytokines, neurotrophins, and other apoptosis-related factors in the nigrostriatal pathway in postmortem PD brains initially by using the enzyme-linked immunosorbent assay (ELISA; Mogi and Nagatsu, 1999; Mogi et al., 2000; Nagatsu, 2002b; Nagatsu et al., 1999, 2000a, b). Our results are shown in Table 2. We further measured mRNA levels by RT-PCR, and also identified cytokine production by immunohistochemistry at the cellular level (Imamura et al., 2003, 2005; Sawada et al., 2006). We obtained the first ELISA evidence for a marked increase in the level of TNF-α in the brain (striatum) and lumbar CSF (Mogi et al., 1994). This finding was supported by the result of an immunohistochemical study by Boka et al. (1994).

We found that the levels of the following cytokines and apoptosis-related factors in the nigrostriatal pathway, and/or in ventricular and lumbar CSF were elevated: TNF-α, IL-1β, IL-2, IL-4, IL-6, EGF, TGF-α, bFGF, TGF-β1, TNF-β2, Bcl-2, soluble FAS, TNF-α receptor R1 (p55), caspases 1, and 3. We also found decreased levels of neuroprotective neurotrophins, BDNF and NGF, in the substantia nigra. These data on changes in the levels of cytokines in human PD brains were also supported by the results obtained from animal models of PD such as MPTP-treated mice (Mogi et al., 1998) and PD rats produced by injecting 6-hydoxydopamine (Mogi et al., 1999).

Studies on cytokines at the cellular level in the postmortem PD brain: immunohistochemistry and mRNA levels measured by RT-PCR

Inflammatory changes called neuroinflammation, most probably induced by activated microglia, in PD brains have been reported by us and other workers (Angrade et al., 1997; Hirsch et al., 1999, 2003; Jellinger, 2000; McGeer et al., 1988; McGeer and McGeer, 1995; Mogi and Nagatsu, 1999; Nagatsu et al., 1999; Nagatsu and Sawada, 2005; Rogers and Kovelowski, 2003; Sawada et al., 2006). We assume that activated microglia are present in the PD brain to produce pro-inflammatory cytokines and neuroinflammation, ultimately promoting death of dopamine neurons in the substantia nigra. Imamura et al. (2003) of our group identified by Western blot analysis TNF-α and IL-6 proteins in the PD brain. By double immunofluorescence staining, they also proved that ICAM-I- and LFA-1-positive MHC class II-bearing activated microglia in the putamen from sporadic PD patients had produced TNF-α and IL-6 proteins.

Activated microglia and neuro-infammation are observed not only in postmortem brains of patients with sporadic PD, but also in brains of patients with PD caused by MPTP (Langston, 1999) and in MPTP-PD monkeys years after MPTP exposure (McGeer et al., 2003). The question is whether these activated microglia are neuroprotective or neurotoxic toward the nigro-striatal dopamine neurons. Based on the *in vitro* finding of a toxic change from a neuroprotective microglial clone to a toxic one by transduction with HIV-1 Nef protein, resulting in increased NADPH oxidase activity (Vilhardt et al., 2002) and on neuropathological findings of the presence of neurotoxic and neuroprotective subsets of activated microglia in the brains of PD and Lewy body disease (LBD) patients by Imamura et al. (2003, 2005), Sawada has hypothesized that activated microglia may be neuroprotective at least in the initial early stage and may later become neurotoxic by a toxic change during the progression of PD, AD, or other neurorodegenerative diseases (Sawada et al., 2006). This microglia-toxic change hypothesis, if correct, would be expected to be useful for developing drugs against PD. Anti-inflammatory drugs, which are speculated to be useful for the treatment of PD, may inhibit